

AMERICAN UNIVERSITY OF BEIRUT

EFFECT OF SILICA ON THE PROPERTIES OF
POLYVINYL ALCOHOL NANOCOMPOSITE MEMBRANES

by
NADINE MOHAMMAD NAJJARINE

A thesis
submitted in partial fulfillment of the requirements
for the degree of Master of Science
to the Department of Nutrition and Food Science
of the Faculty of Agriculture and Food Sciences
at the American University of Beirut

Beirut, Lebanon
May 2014

AMERICAN UNIVERSITY OF BEIRUT

EFFECT OF SILICA ON THE PROPERTIES OF
POLYVINYL ALCOHOL NANOCOMPOSITE MEMBRANES

by
NADINE MOHAMMAD NAJJARINE


Approved by:

Dr. Mohammad Abiad, Assistant Professor
Department of Nutrition and Food Science




Advisor

Dr. Zeina Kassaify, Associate Professor
Department of Nutrition and Food Science



Member of Committee

Dr. Houssam El-Rassy, Associate Professor
Department of Chemistry



Member of Committee

Date of thesis defense: May 5, 2014

AMERICAN UNIVERSITY OF BEIRUT

THESIS, DISSERTATION, PROJECT RELEASE FORM

Student Name: _____ Najjarine _____ Nadine _____ Mohammad _____
Last First Middle

Master's Thesis Master's Project Doctoral Dissertation

I authorize the American University of Beirut to: (a) reproduce hard or electronic copies of my thesis, dissertation, or project; (b) include such copies in the archives and digital repositories of the University; and (c) make freely available such copies to third parties for research or educational purposes.

I authorize the American University of Beirut, **three years after the date of submitting my thesis, dissertation, or project**, to: (a) reproduce hard or electronic copies of it; (b) include such copies in the archives and digital repositories of the University; and (c) make freely available such copies to third parties for research or educational purposes.

_____ 13-5-2014 _____

Signature

Date

This form is signed when submitting the thesis, dissertation, or project to the University Libraries

Date

ACKNOWLEDGMENT

I owe my sincere gratitude to my advisor, Dr. Mohammad Abiad for his everlasting support, for all the resources he put at my disposal, for his encouragement and his patience.

I would like to thank Dr. Houssam El-Rassy and Dr. Zeina Kassaify for their guidance and support throughout my experimental work.

Appreciation is also extended to Dr. Youssef Mouneimneh and Dr. Houssam Cheaib and all colleagues, lab technicians who are too numerous to count.

I would like to thank my supporting and loving mother Nada Najjarine and my family for their blessings, endless love and care, for their patience and support at all times. Thank you my husband, Ahmad El Abed, for your ongoing patience and support.

Finally, I would like to dedicate my work to my deceased father Mohammad Najjarine who always used to support me.

AN ABSTRACT OF THE THESIS OF

Nadine Mohammad Najjarine for Master of Science
Major: Food Technology

Title: The Effect of Silica on the Properties of Polyvinyl Alcohol Nanocomposite Membranes

The sol-gel process is a promising approach for the preparation of nanocomposite films in the presence of templates. The hybrid nanocomposites formed by the sol-gel technique are an emerging ongoing field of exploration in materials science. These nanocomposites form an interesting approach because they exhibit properties of both the organic and inorganic part of the hybrid mixture such as good permeability, selectivity, mechanical strength and thermal and chemical stability. Polyvinyl alcohol (PVA) are being used as the organic polymer part of the composites due to its various biomedical applications such as joint replacement, and controlled drug-releasing devices. In this presented work, polyvinyl alcohol has been used as the organic part of the synthesized nanocomposites. As for the inorganic part of the nanocomposites, colloidal silica, ethyl trimethoxysilane, isobutyl trimethoxysilane, propyl trimethoxysilane and octyl trimethoxysilane have been employed. Colloidal silica was used as the precursor for silica. All the resultant nanocomposites were optically clear. Scanning electron microscopic analyses proved the existence of silica nanoparticles that were uniformly embedded in the organic matrix. Thermal properties of the hybrid nanocomposites were studied using TGA and DSC, proving that the higher presence of silanes enhanced the T_g , T_m and the decomposition temperature of polyvinyl alcohol.

Keywords: sol-gel; nanocomposites; PVA; silanes; T_g ; T_m ; DSC;TGA

CONTENTS

ACKNOWLEDGMENT.....	v
ABSTRACT.....	vi
LIST OF TABLES.....	ix
LIST OF FIGURES.....	ix

Chapter

1- INTRODUCTION.....	1
1. Composite Membrane.....	1
2. Principles of the Sol-Gel Technique	2
3. Silica.....	6
4. Polyvinyl Alcohol	8
2-METHODOLOGY.....	12
1. Materials.....	12
2. Methods.....	12
2.1 Polyvinyl alcohol (PVA) synthesis.....	12
2.2 Preparation of hybrid composites by sol-gel technique.....	13
3. Characterization.....	13
3.1. Scanning electron microscopy (SEM).....	13
3.2 Fourier transform infrared/Attenuated Total Reflectance(FTIR/ATR)...	14
3.3 Thermogravimetric analysis (TGA).....	14
3.4 Differential Scanning Calorimetry (DSC).....	14

3.5 Water Vapor Permeation.....	15
3.6 Data analysis.....	16

3-RESULTS AND DISCUSSION.....17

1. Scanning electron microscopy	17
2 Fourier transform infrared/Attenuated Total Reflectance(FTIR/ATR)	22
3. Thermogravimetric analysis.....	26
4. Differential Scanning Calorimetry	32
5. Water Vapor Permeation.....	35

4- CONCLUSION.....38

REFERENCES.....39

List of Tables

	Page
Table 1 Typical properties of PVOH films compared to other traditional film materials.....	10
Table 2 Glass transition and melting temperatures means of PVA/alkoxysilane nanocomposites.....	34
Table 3 WVTR means of PVA/alkoxysilanes (vol.3) nanocomposites	35
Table 4 WVTR means of PVA/alkoxysilanes (vol.1) nanocomposites.....	36
Table 5 Permeability means of PVA/alkoxysilane nanocomposites	37

List of Figures

		Page
Figure 1	SEM image of PVA-Silica with IsobutylTMS Film (vol.3).....	18
Figure 2	SEM image of PVA-Silica with IsobutylTMS Film (vol.1)	19
Figure 3	SEM image of PVA Film.....	20
Figure 4	SEM image of PVA Film	21
Figure 5	FTIR/ATR spectra for films of a) PVA+ Silica; b) PVA.....	23
Figure 6	FTIR/ATR spectra for films of c1) PVA + EthylTMS (vol.3); c2) PVA + PropylTMS (vol.3); c3) PVA + IsobutylTMS (vol.3); c4) PVA + OctylTMS (vol.3).....	24
Figure 7	FTIR/ATR spectra for films of c5) PVA + EthylTMS (vol.1); c6) PVA + PropylTMS (vol.1); c7) PVA + IsobutylTMS (vol.1); and c8) PVA + OctylTMS (vol.1).....	24
Figure 8	FTIR/ATR spectra for films of d1) PVA-Silica + EthylTMS (vol.3); d2) PVA-Silica + PropylTMS (vol.3); d3) PVA-Silica + IsobutylTMS (vol.3); d4) PVA-Silica + OctylTMS (vol.3).....	25
Figure 9	FTIR/ATR spectra for films of d5) PVA-Silica + EthylTMS (vol.1); d6) PVA-Silica + PropylTMS (vol.1); d7) PVA-Silica + IsobutylTMS (vol.1); and d8) PVA-Silica + OctylTMS (vol.1).....	25
Figure 10	TGA thermograph of PVA film.....	28
Figure 11	TGA thermograph of PVA+ Silica film.....	29
Figure 12	TGA thermograph for films of c1) PVA + EthylTMS (vol.3); c2) PVA + PropylTMS (vol.3); c3) PVA + IsobutylTMS (vol.3); c4) PVA + OctylTMS (vol.3).....	30
Figure 13	TGA thermograph for films of c5) PVA + EthylTMS (vol.1); c6) PVA + PropylTMS (vol.1); c7) PVA + IsobutylTMS (vol.1); and c8) PVA + OctylTMS (vol.1).....	30
Figure 14	TGA thermograph for films of d1) PVA-Silica + EthylTMS (vol.3); d2) PVA-Silica + PropylTMS (vol.3); d3) PVA-Silica + IsobutylTMS (vol.3); d4) PVA-Silica + OctylTMS (vol.3).....	31
Figure 15	TGA thermograph for films of d5) PVA + EthylTMS (vol.1); d6) PVA + PropylTMS (vol.1); d7) PVA + IsobutylTMS (vol.1); and d8) PVA + OctylTMS (vol.1).....	31

ABBREVIATIONS

%	Percentage
MF	Microfiltration
UF	Ultrafiltration
NF	Nanofiltration
RO	Reverse Osmosis
ED	Electrodialysis
ME	Membrane Electrolysis
DD	Diffusion Dialysis
GS	Gas Separation
VP	Vapor Permeation
PV	Pervaporation
MD	Membrane Distillation
MC	Membrane Contactors
PVA/PVOH	Polyvinyl Alcohol
OH	Hydroxyl Group
Si(OR) ₄	Semi-Metal Alkoxides
TEOS	Tetraethoxysilane/ Tetraethylorthosilicate/ Silicon Tetraethoxide
pH	Power of Hydrogen
SN	Nucleophilic Substitution
SiO ₂	Silicon Dioxide
N	Coordination Number
Z	Oxidation State
SEM	Scanning electron microscopy
HSD	Honestly Significance differences
TGA	Thermal gravimetric analysis
FTIR/ATR	Fourier Transform Infrared/ Attenuated Total Reflectance

WVTR	Water Vapor Transmission Rate
T _g	Glass Transition Temperature
T _m	Melting Temperature
CGC	Critical Gel Concentration
H ₂ O	Water
nm	Nanometer
EthylTMS	Ethyl Trimethoxysilane
PropylTMS	Propyl Trimethoxysilane
IsobutylTMS	Isobutyl Trimethoxysilane
OctylTMS	Octyl Trimethoxysilane
CS	Colloidal Silica
HCl	Hydrochloric Acid
NH ₄ OH	Ammonium Hydroxide
M	Molar
RH	Relative humidity
mg	Milligram
min	Minute
cm	Centimeter
EDX	Energy Dispersive X-ray Spectroscopy
Pa	Pascal
M	Meter
g	Gram
sec	Second
vol.	Volume

CHAPTER 1

INTRODUCTION

1. Composite Membranes

Recent studies on polymers used in the synthesis of hybrid organic-inorganic nanocomposite films have grabbed the attention of scientists. In these hybrid nanocomposites, the inorganic fillers strengthen the organic polymers. Nanocomposites are novel type of materials that display ultrafine phase measurements, typically in the range of 1–100 nm. Fortunately, there have been good reviews on this topic that helped formed a baseline for further researches in this domain (JE., 2006; Z & JE, 2001). The objective behind synthesizing organic-inorganic nanocomposites (Hillmyer, Lipic, Hajduk, Almdal, & Bates, 1997; Lipic, Bates, & Hillmyer, 1998) relies in linking the microstructures and intrinsic properties of the diverse materials making up the nanocomposites. Hence, properties that cannot be attained using either constituent separately will be achieved.

Membrane science and technology have been the lead in the innovation of products for sustainable manufacturing development. These membranes were at first used as analytical method for chemical and biomedical laboratories. Later on, they entered the industrial field with noteworthy technical characteristics. Nowadays, these membranes are used in the food and drug industries and as gas separators in the petrochemical field (Baker, 2004; Noble & Stern, 1995).

A synthetic membrane acts as barrier for the components of the product. It prohibits the transfer of the chemical species in precise way. This membrane can be found in solid, liquid, homogenous, heterogeneous, isotropic or anisotropic state. Also, it can be positively, negatively

or neutrally charged or bipolar as well. The thickness of this membrane can vary between fractions of micrometer and millimeters. Hence, this membrane can display different properties depending on its structure and the function (Mulder, 1996). Membranes demonstrate a variety of tools. They are used for separation of particles from solution, toxins from blood and a mixture of different gases. This number of applications is growing up to date. Two generations of membranes can be illustrated. The first one includes membrane processes are microfiltration (MF), ultrafiltration (UF), nanofiltration (NF), reverse osmosis (RO), electrodialysis (ED), membrane electrolysis (ME), diffusion dialysis (DD), and dialysis, while the second one includes gas separation (GS), vapor permeation (VP), pervaporation (PV), membrane distillation (MD), membrane contactors (MC) and carrier mediated processes. Through the membranes, passive transport occurs. This is as a result of a driving force and a variation in chemical gradient across the membrane. This chemical gradient can be concentration, pressure, or electrical field. The membrane separation processes can be categorized into three classes depending on their driving forces that are engaged in the separation. Despite that each process has a different mechanism, yet they all have the membrane in common. The membrane acts as the heart of each membrane process. On a commercial scale, large membrane areas are mostly required. A module is the smallest component into which the membrane area is set. It is the innermost fraction of a membrane setting up. Between 1960s and 1970s, the development of the technology was emphasized on the fabrication of low cost membrane modules (Baker et al., 1991).

2. Principles of the Sol-Gel Technique

To synthesize these nanocomposite films, sol-gel method has been employed (Mark, Lee, & Biancini, 1995; Strejko, Jasiorski, Ucyk, & Maruszewski, 2003). Through the sol-gel process,

innovative opportunities for making new polymer-metal oxide hybrid materials have been established. Sol-gel has been used a manufacturing procedure for homogenous inorganic glasses. However, sol-gel is used now as a method to produce a range of organic-inorganic hybrid materials (Bahulekar, Prabhune, SivaRaman, & Ponrathnam, 1993; Hoh, Ishida, & Koenig, 1990; Novak & Davies, 1991; Zarzycki, 1997). Sol-gel chemistry in polymers is considered to be a flexible technique since it controls the nature of the interface of the organic-inorganic hybrid composites. The interaction, size and shape of these component phases contribute to the films various properties. Additionally, sol-gel method possesses a wide field of applications such as catalysis (St. Pierre & El Sayed, 1987), luminescence (Wen & Wilkes, 1996), water perm selective membrane, immobilization carriers for a biocatalyst (Nakane, Yamashita, Iwakura, & Suzuki, 1999), and nonlinear optical properties (Kobayashi, 1989).

The sol-gel technique is a two- step technique including the synthesis of a sol at first which is then followed by the creation of a gel. Next, the gel is left to dry in order to eliminate the organic solvents. This will form a porous network. The sol-gel method is an approach where the materials synthesized are derived from hydrolysis of certain molecular precursors. These precursors are usually metal or semi-metal alkoxides such as $(\text{Si}(\text{OR})_4)$ that reveals high reactivity. To form these metal oxides, the sol-gel technique follows the two consecutive reactions, hydrolysis and polycondensation (Brinker & Scherer, 1990). This technique follows mild conditions which permits the insertion of organic molecules inside an inorganic network (H.-H. Huang, Orlor, & Wilkes, 1985; Sanchez, Ribot, & Lebeau, 1999; Schmidt, Scholze, & Kaiser, 1982; Sur & Mark, 1985). Several parameters regulate these chemical procedures and control the homogeneity or heterogeneity of the derived nanostructures (Schubert, 1996).

Generally, the area, porosity, pore volume and pore size distributions of the material are characteristics that are majorly controlled by the sol-gel process.

Using sol-gel approach, oxide films can be prepared from precursors containing alkoxysilyl groups where it combines metal alkoxide precursors of formula $[M(OR)_n]$ and water, M being a network of an inorganic element and R being an alkyl group. Sol-gel technique is a continuous process formed of two fundamental steps: Hydrolysis and condensation of the metal alkoxide. This yields homogeneous sol-gel mixtures where inorganic network embedded within the polymer matrix (H. H. Huang, Orlor, & Wilkes, 1987). Studies showed that integrating silica factor from silica precursors into organic polymers forms consistent nanocomposites with improved separation performance (Gomes, Nunes, & Peinemann, 2005; Y.-L. Liu, Su, Lee, & Lai, 2005; Peng et al., 2005; Uragami, Matsugi, & Miyata, 2005; Uragami, Okazaki, Matsugi, & Miyata, 2002a; Yan, Li, & Xiang, 2005). Hydrogels are defined as network of polymer chains that are hydrophilic and highly absorbent. Hydrogels that are formed by chemical or physical crosslinking constitute a distinctive class of polymers that requires significant quantity of water while sustaining their shape. In tissue engineering field, hydrogels that are formed from natural polymers have been employed. However, such hydrogels have limitations, thus new approaches to modify these polymers and use synthetic polymers have been employed.

The sol phase of the sol-gel material is explained as a flowing fluid and the dispersions of colloidal particles in a liquid, whereas the gel phase is the non-flowing section. The term "gel" holds a variety of combined substances that are classified in four categories (Flory, 1969). These four categories are: (1) ordered lamellar assemblies, (2) Polymers with covalent networks that are completely disordered, (3) polymer networks that are made through physical aggregation, and are predominantly disordered; (4) and particular disordered structures. Colloids are defined

as solid particles having diameters of 1-100nm (Davies & Rideal, 1963). Above the critical gel concentration (CGC) of a polymer, the gel phase is produced. The CGC is usually inversely associated to the polymers molecular weight. One of the prerequisites to determine gelation is the development of the physical junctions in the system. These junctions should be adequately strong in regards to the dissolving forces of the solvent that are driven by entropy. The gelation of these organic polymer solutions follows a number of mechanisms (Finch, 1983; Guenet, 1992). Optimizing the reaction parameters is an essential issue because of the different miscibility and condensation patterns of the reaction components. These parameters are the pH of the solution, the mole ratio of Si, polymer and H₂O, catalysts, solvents and reaction temperature. Different kinds of organic polymers such as polyvinyl alcohol (PVA), polymethylmethacrylate, and bisphenol (A) polycarbonate form these composites. In the early 1990s, the interaction of methyl methacrylate (Yen, Dachuan, & Bakthavatchalam, 1992), styrene (Yen Wei, Yang, Tang, & Hutchins, 1993) and acrylonitrile (Y Wei, Yang, & Tang, 1993) with silica using the mentioned approach generates transparent materials where the organic phase binds to the inorganic phase and prohibits the existence of macro-phase separations were demonstrated.

Many soluble long-chain polymers can be modified to insoluble gels by adequate cross-linking of the molecules. Even if the molecular weight distribution is modified, a gel cannot be formed by a small degree of cross-linking. However, higher degrees of cross-linking yield a heterogeneous material constituted of the insoluble part being the gel and the soluble part being the sol. Integrating a silicate matrix into an organic polymer, using the sol-gel technique, has several beneficial applications. For instance, the polymer/silicate composite electrolytes hold high ionic conductivity and sufficient mechanical strength to isolate anode from cathode

(Harrup, Wertsching, & Stewart, 2003). One significant aspect in this field of study has been analyzing the hydrogel behavior of these composites.

3. *Silica*

Silicon dioxide, also known as silica, is a chemical compound that is constituted of a dioxide of silicon. It has the chemical formula SiO_2 . Silica that is highly pure is extensively used in industries. It has many roles to display. It can act as a catalytic support, filler, or waveguide. It is also used in fused silica wares and in optical glasses (Mokoena, 2005). Moreover, silica tends to be used as thermal and acoustic insulators. To obtain pure silica, controlled hydrolysis of silicon alkoxides shall be performed (Calvin H Bartholomew, Pannell, & Butler, 1980; Y.-J. Huang & Schwarz, 1987; Sinfelt, Cusumano, Burton, & Garten, 1977; Vannice, 1975). The (+4) oxidation state of silicon ($z = 4$) is what makes silicon special. This oxidation state of silicon is in naturally occurring systems (Sinfelt et al., 1977). The coordination number of silicon, (N), is usually 4. Silicon is generally less electropositive in comparison to aluminum and transition metals (Duvenhage, Espinoza, Coville, Delman, & Froment, 1994).

This is an advantage to silicon since it helps silicon be less susceptible to nucleophilic attack (Calwin H Bartholomew & Guzzi, 1991). Hence, Si-C bonds are hydrolytically stable and this allows a facilitated fixing of functional organic groups (Jager & Espinoza, 1995). The kinetics of hydrolysis and condensation are affected by these factors. These factors decrease the rate of their kinetics relative to alumina and transition metal alkoxide systems (Calwin H Bartholomew & Guzzi, 1991). Therefore, acid or base catalysts are commonly used in silicon-based alkoxide systems. In an acidic medium, the hydrolysis rate is much higher compared to that of condensation. Consequently, the acid catalysts stimulate the formation of polymer-like molecules

at the beginning of the reaction. However, base catalyst shows higher condensation rate relative to hydrolysis (Bukur & Lang, 1999). This base catalyst helps in formation of a tightly closed cluster growth that in its turn direct to dense silica colloidal configurations (Calvin H Bartholomew & Guzzi, 1991; Butt, Schwartz, Baerns, & Malessa, 1984; Dry, 1982; Z.-T. Liu, Li, Zhou, & Zhang, 1995).

Silica acts as metal catalyst support in reactions like the Fischer-Tropsch reaction. In addition, silica actively takes part in few oxidation reactions, for instance methanol oxidation (Calvin H Bartholomew, 1991), methane to formaldehyde oxidation (Forzatti, Buzzi-Ferraris, Morbidelli, & Carra, 1984) and ammoxidation (Oudar, 1985). Sol-gel approach fabricates amorphous silica (Guzzi, Schay, Matusek, & Bogyay, 1986; Ishihara, Eguchi, & Arai, 1987). The Silicon dioxide reacts with metal oxides or combination of oxides to obtain silicates. During the reaction, the Si-O-Si bonds in silica are broken successively. The chief advantages relying in preparing silica from sol-gel method are the obtained compositional homogeneity and low required processing temperatures. In this reaction, the alkoxide dissolve in alcohol and are hydrolyzed by adding water in an acidic, neutral or basic medium. This gives the SiO_2 product.

Silica has the ability to undergo not less than 22 modifications from crystalline to amorphous forms. This gives the substance SiO_2 a great interest. Silica shares excellent mechanical, thermal and optical properties. Silicon precursors are used in the sol-gel process among other silicon alkoxides. Silica has various fields of applications such as in chromatography, thermal isolation, catalysis, support for catalysts, dehydration, gelation of liquids, polymer reinforcement, liquid crystal posting, fluidization of powders, and more recently support for enzyme immobilization (Walcarius, 1998). These silica nanoparticles can exist in powder or colloid forms. Silica by nature is found in solid state and they are crystalline. However

silica can be prepared by synthetic processes, but this renders them amorphous shape. Silica exhibits several properties such as large surface area and smooth nonporous surface. Also, alkoxysilanes have shown promising applications when co-interacting with polymers. These alkoxysilanes can be used in coating applications as in fillers for surface treatments; thus improving the coating integrity (Witucki, 1993). Polymers and silica material show great differences in their properties. This can cause phase separation. Hence, the interfacial interactions between the polymer and the silica critically influence the consequential material.

4. Polyvinyl Alcohol

Polyvinyl alcohol, which can be symbolized by PVA or PVOH, is derived from the vinyl acetate product. To polymerize vinyl acetates, radical initiator and methanol acting as solvent and chain transfer mediator are used. In order to control the molecular weight of the product of the reaction, which is polyvinyl acetate, methanol and both the amount and type of initiator are selected. Next, the polyvinyl acetate is hydrolyzed with methanol and sodium hydroxide to produce polyvinyl alcohol. Temperature, time and concentration of sodium hydroxide are the parameters that govern the degree of hydrolysis of the reaction. However, residual acetyl group, distribution, branching, average length and tacticity are other parameters that have less impact on the properties of PVA than do the molecular weight and degree of hydrolysis (Lehtinen, 2000).

PVA has a notable adhesion to fillers and fibers and thus can be used as a sizing agent. Also, PVA strengthens the surface and dimensional stability of sized paper and paperboards. PVA improves other mechanical and barrier properties, which help reduce water adsorption in PVA sized papers. Being a great binder between fiber and particles, PVA decreases the dusting in printing.

Polyvinyl alcohol has been utilized as a cross-link to produce ultra-thin films. This crosslinking is achieved by heat, radiation treatment or with organic treatment. Polymeric membranes have grabbed great attention due to their diverse applications and research has been done on improving these membrane materials. PVA is extensively used as battery separators, pervaporation membranes and dialyzer diaphragms. PVA is a promising polymeric material. It can be used in the making of fibers, films, adhesives and papers. It also protects surface coating on top of the nanocomposite membranes. PVA is a crucial hydrophilic vinyl polymer. Therefore, it is an outstanding membrane material for the fabrication of hydrophilic membranes. It is synthesized through partial or complete hydrolysis of polyvinyl acetate (Shaw, 1980). PVA has high affinity to water because its hydroxyl group can form strong hydrogen bonds between intra- and intermolecular hydroxyl groups. Depending on both the degree of hydrolysis and the polymer chain length, the solubility of water is affected. However, being hydrophilic, PVA is prompt to degradation and elimination in the unmodified structure. Hence, PVA shall be modified to present long term stability. To overcome this drawback, PVA can be chemically modified to obtain new characteristics and widen its range of application (Lappalainen, 2008). Table 1 summarizes typical properties of PVOH films compared to other traditional film materials.

Table 1: Typical properties of PVOH films compared to other traditional film materials (Hodgkinson & Taylor, 2000)

Property	PVOH
Clarity (light transmitted) (%)	60-66
Gloss (light reflected) (%)	81.5
Tear strength (Elmendorf) (N.mm ⁻¹)	147-834
Tensile strength (MN.m ⁻²)	44-64
Elongation at break (%)	150-400

The polyvinyl alcohol (PVA)/silica arrangement has received attention because of the hydrogel behavior of polyvinyl alcohol (Cauich-Rodriguez, Der, & Smith, 1996). Polyvinyl alcohol has been applied in the synthesis of an artificial heart valve stent, membranes (Xiao, Feng, & Huang, 2007), fibers (Hong & Miyasaka, 1994), adhesives (Jenni, Holzer, Zurbriggen, & Herwegh, 2005), coatings (Wang, Fang, Yoon, Hsiao, & Chu, 2006), polymer electrolytes (Jeong, Jo, & Jo, 2006), tissue replacement biomaterials (Oka et al., 1997), and controlled release biomedical material (Stammen, Williams, Ku, & Guldborg, 2001). PVA is best known for its ability in resisting chemical (Yang, Lin, & Wu, 2005), and film forming, processability, availability and biocompatibility. Furthermore, PVA is biocompatible, nonhazardous and reveals negligible cell adhesion and protein absorption (Burczak, Gamian, & Kochman, 1996). However, due to its poor water resistance and deficient mechanical properties, PVA's application have

been limited particularly for tissue replacement biomaterials and wound dressing materials for which tear and impact resistances are necessary (Chang, Kim, & Nam, 2005).

Polyvinyl alcohol is very delicate towards moisture that plasticizes the polymer and diminishes its strength. Most of the previous studies have dealt epoxidised natural rubber polymers with polar groups (Bandyopadhyay, Bhowmick, & De Sarkar, 2004) that are available for interaction with the silanol groups of the inorganic part. Uragami *et al.* (Uragami, Okazaki, Matsugi, & Miyata, 2002b) have presented the formation of hybrid nanocomposites using polyvinyl alcohol and tetraethoxysilane in dimethyl sulphoxide. However, no detailed exploration concerning structure-property relationships of PVA/Colloidal Silica with trimethoxysilanes has been stated. Consequently the current work aims at not only exploring the thermo-mechanical properties of the composites formed from the dispersion of the highly hydrolyzed-grade polyvinyl alcohol in the inorganic colloidal silica part on a nanoscale, but also illustrating the structure-property relationships of the resulting nanocomposites.

CHAPTER 2

Methodology

1. Materials

The polyvinyl alcohol used to synthesize the hybrid nanocomposites was purchased from ACROS Organics (Fair Lawn, NJ, USA). The LUDOX HS-40 colloidal silica 40 wt.% suspension (CS) in H₂O, isobutyl trimethoxysilane (IsobutylTMS), and octyl trimethoxysilane (OctylTMS) were acquired from Sigma Aldrich (St. Louis, MO, USA). Propyl trimethoxysilane (PropylTMS) and ethyl trimethoxysilane (EthylTMS) were purchased from FLUKA (Gillingham, UK). Hydrochloric acid was supplied by Merck (White House Station, NJ, USA) and ammonium hydroxide was bought from Fisher Scientific International, Inc. (Pittsburgh, PA, United States).

2. Methods

2.1 Polyvinyl alcohol (PVA) synthesis

A 5% polyvinyl alcohol solution was prepared from 87% hydrolyzed PVA and distilled water. The PVA was dissolved in distilled water and heated to 85°C while continuously stirring for 30 min to ensure complete dissolution. The 5% PVA solution was then left to cool down at room temperature.

2.2 Preparation of hybrid composites by sol-gel technique

In this study, the molar ratio of colloidal silica (CS) with respect to the ratio PVA was used. Distilled water acting as the solvent, CS, alkyl trimethoxysilanes and 0.2M HCl were added consecutively while stirring at room temperature. After 10min, the temperature of the solution was raised to 85°C and PVA was added while stirring. Consequently, after 2 hours, 0.5M NH₄OH was added and the solution was casted on polystyrene dishes and placed in an environmental chamber with a relative humidity of 85% over potassium chloride salts for 10 days. Two sets (vol.1 and vol. 3) of nanocomposites of the same constituents but with different proportions were prepared. Set 1 (vol.1) had the following constituents: water, silica, HCl, PVA and NH₄OH. Set 2 (vol.3) had the same constituents of set 1 but their quantities were three times the quantities of set 1. The quantity of water was the same in both sets. Afterwards, the obtained nanocomposite films were placed in a vacuum oven at 60°C for 24 hours before testing.

3. Characterization

3.1 Scanning electron microscopy (SEM)

To study the surface topography of the hybrid nanocomposites, a VEGA 3 LMU SEM (TESCAN, Brno, Czech Republic) equipped with an EDX detector model INCA XMAW 20 (Oxford Instruments, UK) and LaB₆ gun was used. The samples were sputter-coated with platinum (10 nm) by means of an Emscope SC 500 (Emscope Laboratories Ltd, Ashford, UK). SEM photomicrographs were taken at an accelerating voltage of 20 kV.

3.2 FTIR/Attenuated Total Reflectance (FTIR/ATR)

The structure of the hybrid nanocomposites was examined using an iD3 ATR Accessory for the Nicolet™ iS5 Spectrometer (Waltham, MA, USA) sampling technique with an attenuated total reflectance. The spectra were collected in the 4,000 – 600 cm^{-1} range. Samples were run in triplicates.

3.3 Thermogravimetric analysis (TGA)

Thermogravimetric analyses of the organic/inorganic hybrid nanocomposites were done using TG 209 *FI Libra*® - Thermo-Microbalance (Thermogravimetric Analyzer) (NETZSCH, Selb/Bavaria, Germany) was used to perform. The TG 209 *FI Libra*® was coupled with FTIR spectrometer TENSOR™ 27 (Billerica, MA, USA). 5mg samples were heated between 30 and 700°C at a rate of 10°C min^{-1} . The TGA data was analyzed using the *Proteus*® 6.1 software (NETZSCH). Data was collected in triplicates.

3.4 Differential Scanning Calorimeter (DSC)

The various thermal transitions of the hybrid nanocomposites were analyzed using TA Instruments, Q2000 Differential Scanning Calorimeter (TA Instruments, New Castle, DE, USA). 4mg samples were heated between -20°C to 250°C at a rate of 5°C/min. Data was collected in triplicates.

3.5 Water Vapor Permeation

Water vapor permeation units *SHEEN 1003* by Sheen Instruments (*Guildford, Surrey, UK*) were used to measure the water vapor permeation throughout the obtained hybrid nanocomposites. The test specimens were sealed to the open mouth of a test dish containing 3mL distilled water. The assemblies were then placed in a controlled environmental chamber over 0% relative humidity silica gel. The samples were weighed periodically. Water vapor transmission is taken as the slope of the curve divided by the area of the dish opening. The technique used to measure WVTR was a modification of the wet cup method described by the ASTM E 96-95. The WVTR was calculated from the steady-state regression. Thickness measurements with a digital gauge at a minimum of 12 positions on a test specimen were collected.

$$\text{Water vapor transmission rate} = \frac{Q}{A \times t} \quad (\text{eq. 1})$$

WVTR = Water vapor transmission rate (cc/ m². day)

Q = quantity of gas transmitted (cc)

A = Film Area (m²)

t = Time (day)

$$\text{Permeability Coefficient} = \frac{WVTR \times Z}{\Delta P} \quad (\text{eq. 2})$$

Z= Thickness (m)

WVTR= Water vapor transmission rate (cc/ m². day)

ΔP= Partial pressure difference of water vapor across the film (Pa)

3.6 *Data analysis*

Tukey's HSD (Honestly Significant Differences) tests were performed at 95% confidence interval ($\alpha = 0.05$) to determine the significant differences between the means. The analyses were conducted using IBM SPSS software (IBM Corporation, Armonk, NY, USA).

CHAPTER 3

RESULTS AND DISCUSSION

1. Scanning electron microscopy

Morphological characteristics of the nanocomposites obtained were analyzed using SEM. In accordance to the morphological examinations and optical clarity of the films, local silica phase dispersed within the hybrid composite was noticed in PVA+Silica with IsobutylTMS (vol.3) (figure 1). SEM picture for the PVA+Silica with IsobutylTMS (vol.1) in figure 2 confirms the spreading of the inorganic silica phase within the polyvinyl alcohol matrix. It is established that the silica particles yield aggregated configurations in the PVA hybrid nanocomposites. Also, PVA morphology is illustrated in figures 3 and 4. The granules form of the porous PVA designates amorphous behavior which is present in the pure polymer. Voids are present in the structures of PVA. Yet, by introducing silica to the PVA matrix, a collapsed structure is shown. The voids are no longer visible as seen in figures 1 and 2. A decrease in the porosity of PVA is attained.

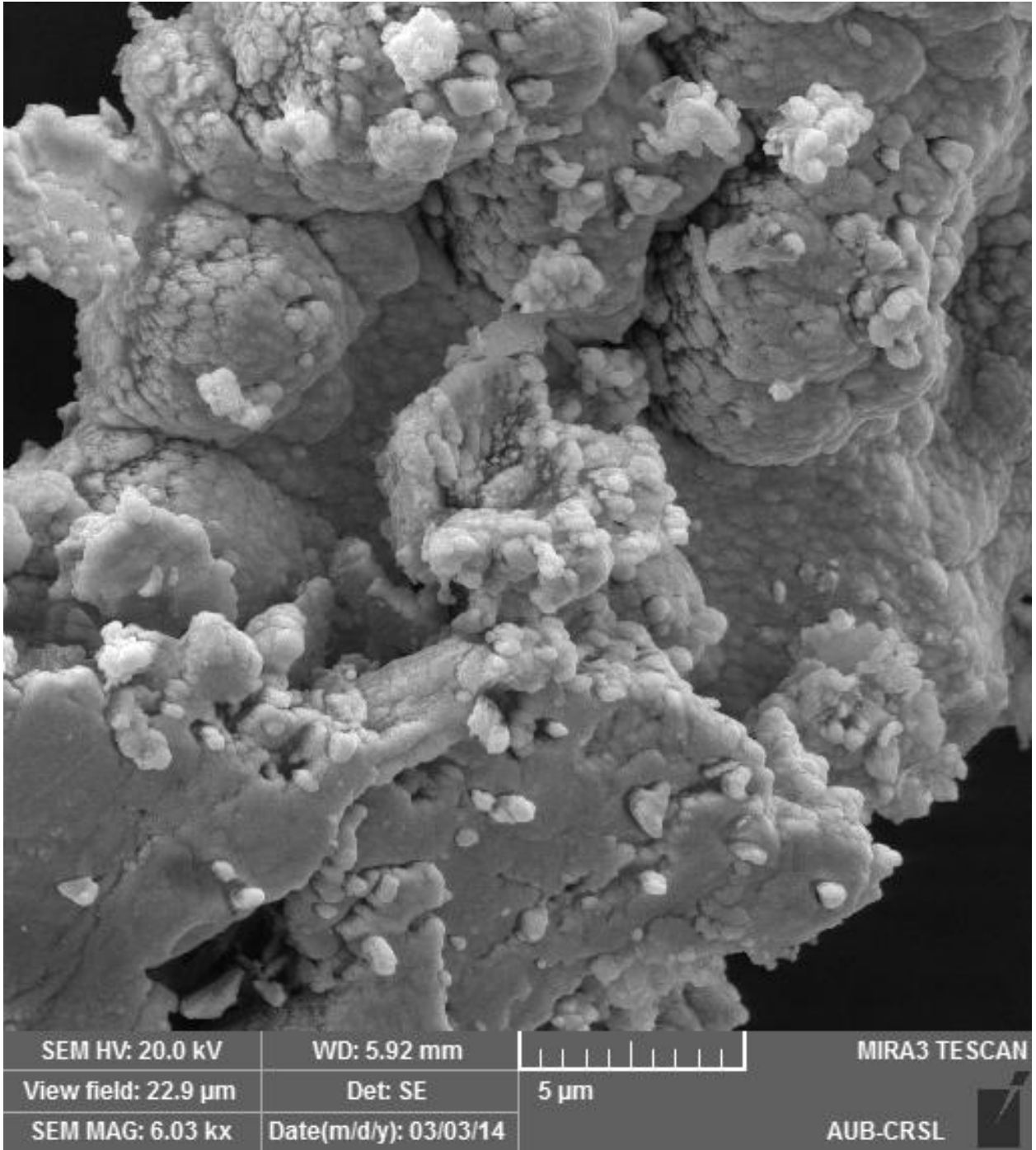


Figure 1: SEM image of PVA-Silica with IsobutylTMS Film (vol.3)

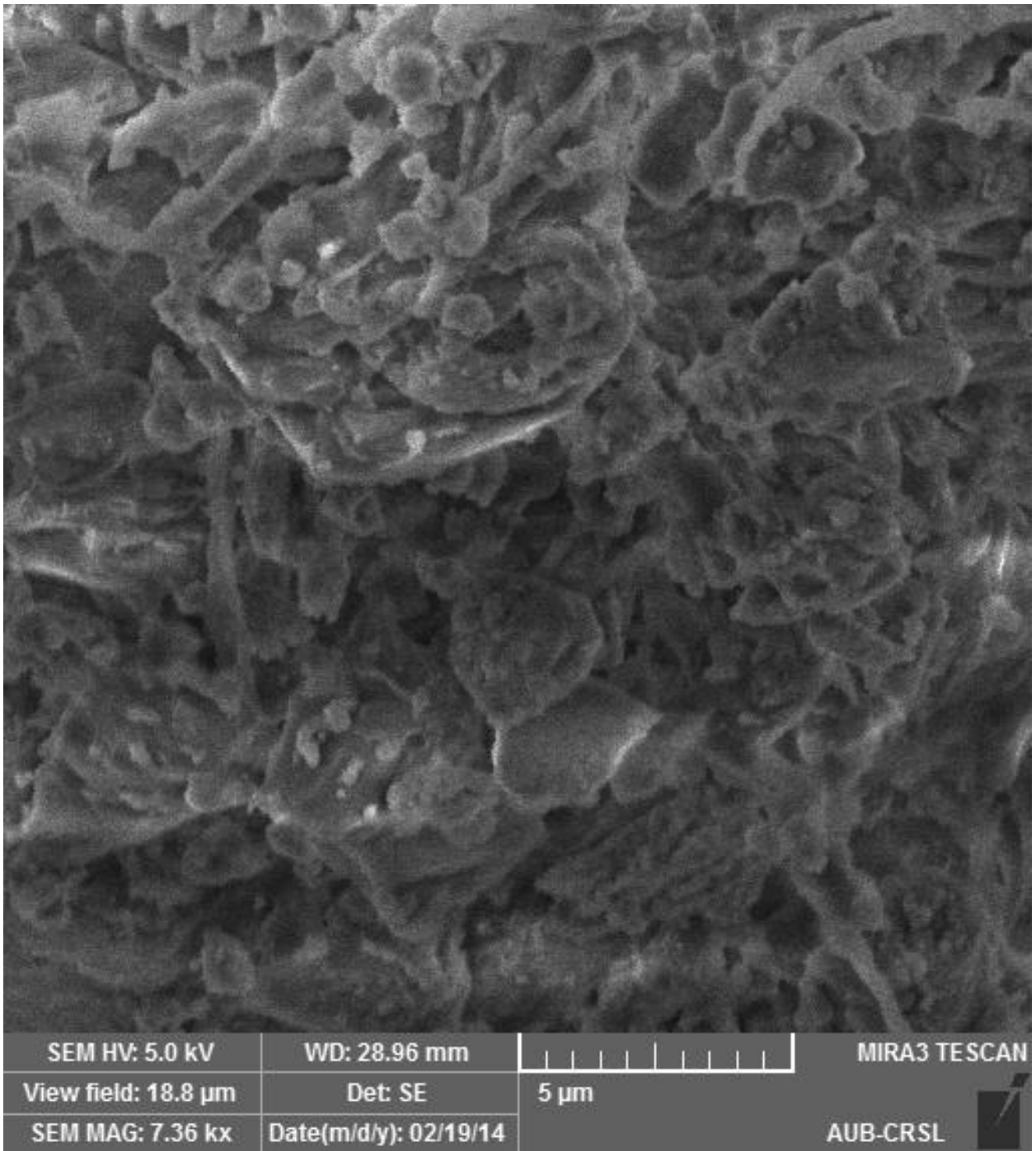


Figure 2: SEM image of PVA-Silica with IsobutylTMS Film (vol.1)

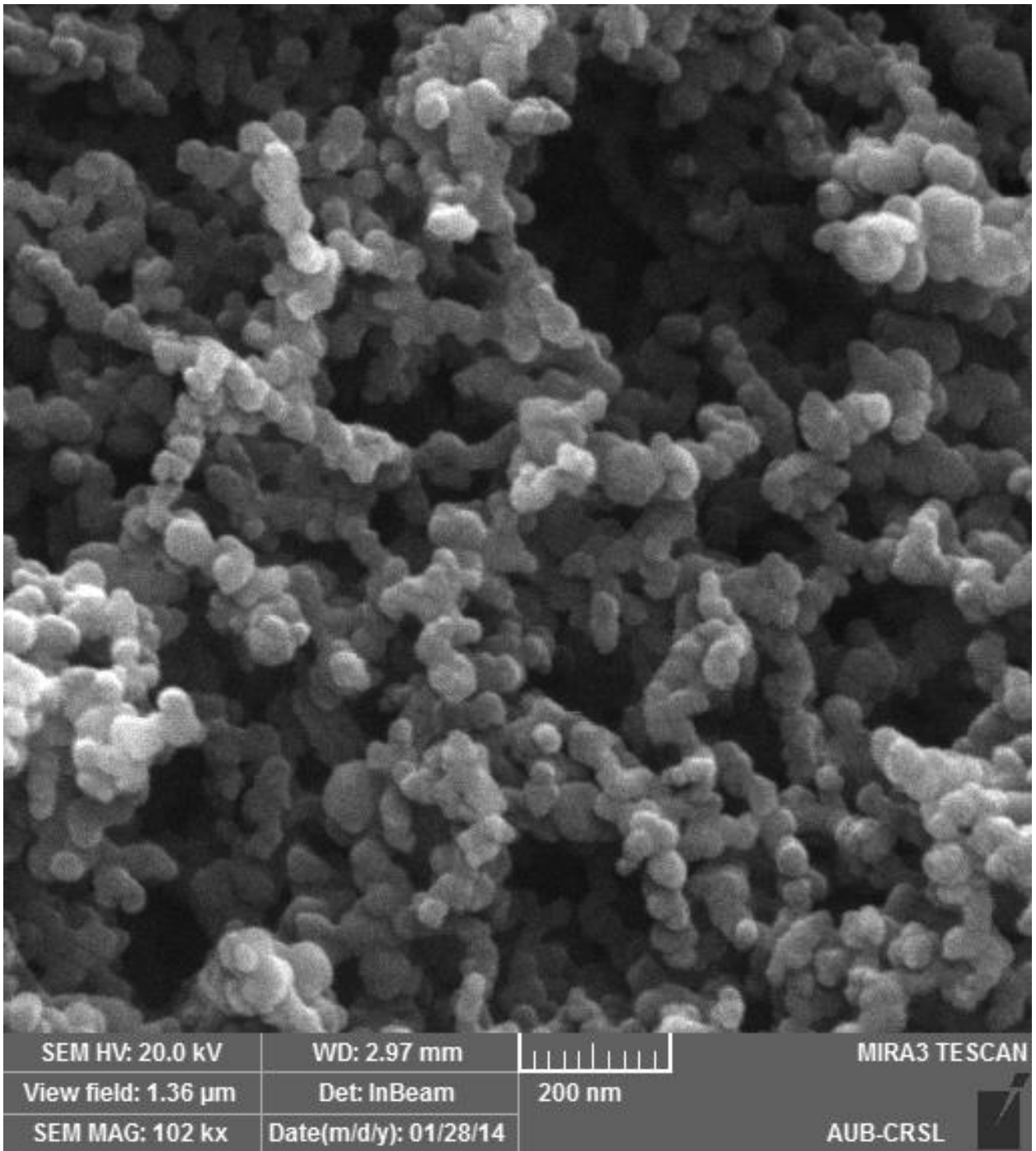


Figure 3: SEM image of PVA Film

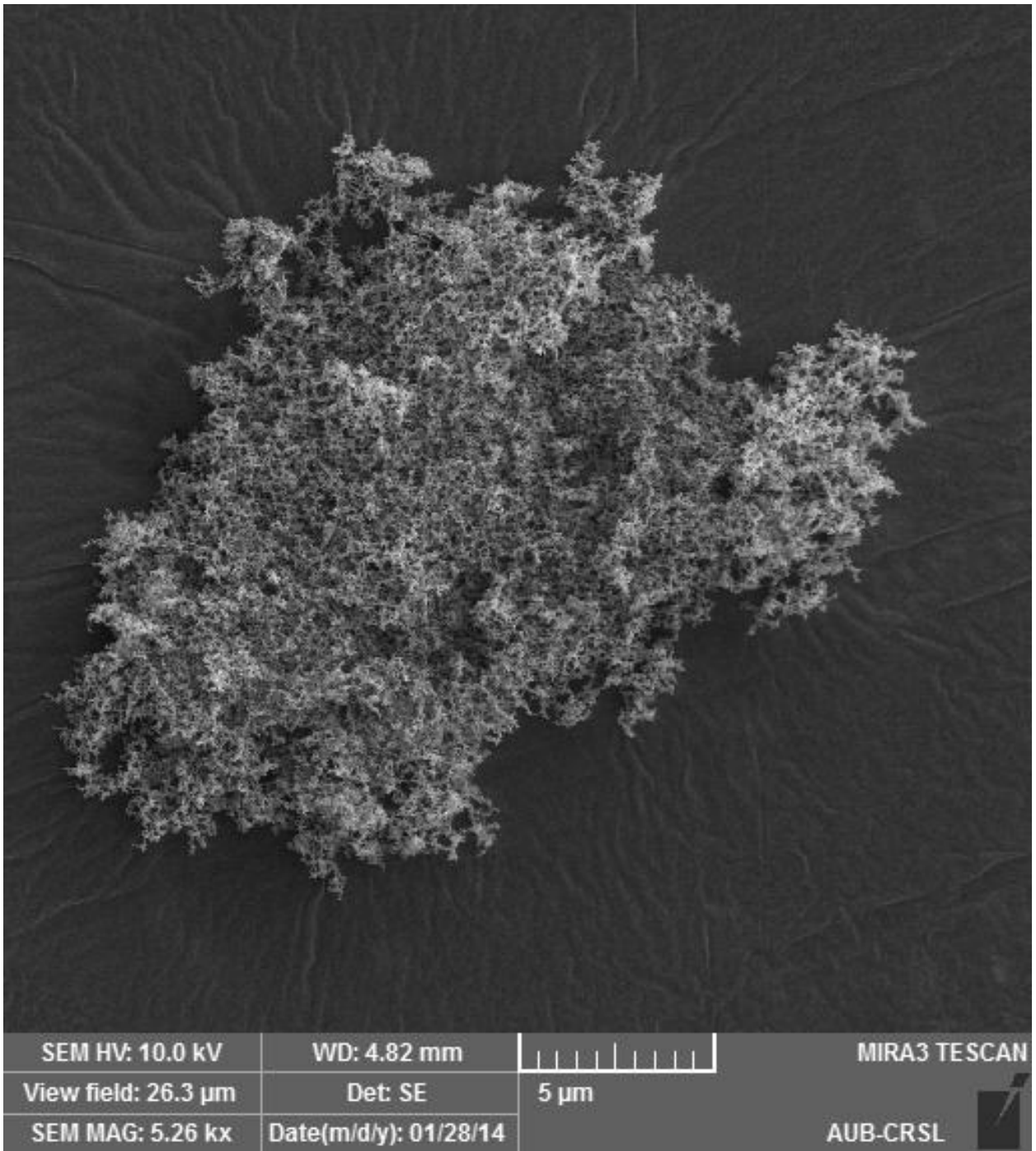


Figure 4: SEM image of PVA Film

2. FTIR/ATR

Figure 5 shows the FTIR-ATR spectra for pure PVA nanocomposite and PVA+Silica nanocomposite. As for figures 6 and 7, different FTIR-ATR spectra of PVA with trimethoxysilane nanocomposites are displayed and of PVA+Silica with trimethoxysilane are presented in figures 8 and 9. The comparison of the FTIR spectra, to verify the existence of both guest and host molecules of the pure PVA nanocomposites and the PVA+Silanes nanocomposites, demonstrates a significant modification in the shape and location of some functional groups. For instance, in figures 6 and 7, Si–O–Si anti symmetric stretching vibration type is recognized at 1180 cm^{-1} and $\nu[\text{CH}_2]$ that's stretching in type is detectable at 2900 cm^{-1} . C-H vibration representing bending or symmetric deformation vibration is noticed at 1250 cm^{-1} (Al-Oweini & El-Rassy, 2009).

Si–O–Si anti symmetric stretching vibration type is found for PVA+Silica nanocomposites only (figure 5). As for PVA with alkoxysilanes nanocomposites, Si–O–Si anti symmetric stretching vibration type recognized at 1180 cm^{-1} is found in higher quantities for PVA with alkoxysilanes nanocomposites (vol.3) than it is for (vol.1). Both figures 8 and 9 show that this Si–O–Si anti symmetric stretching vibration is found in the highest amount for PVA+Silica with trimethoxysilanes (vol.3) as they have the highest amount of silanes in their nanocomposites. Moreover, all of the FTIR/ATR figures show the $\nu[\text{CH}_2]$ vibration, which is detectable at 2900 cm^{-1} . OH bend is detectable in all the present FTIR/ATR figures at 3217 cm^{-1} since all nanocomposites contain PVA.

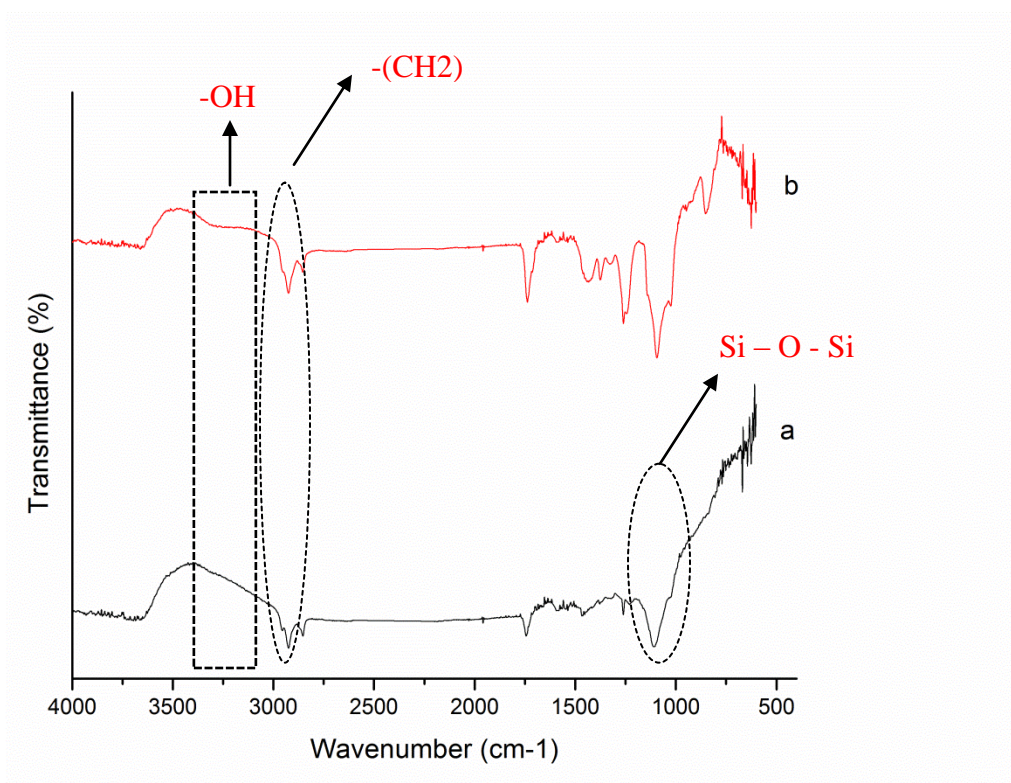


Figure 5: FTIR/ATR spectra for films of a) PVA+ Colloidal Silica; b) PVA

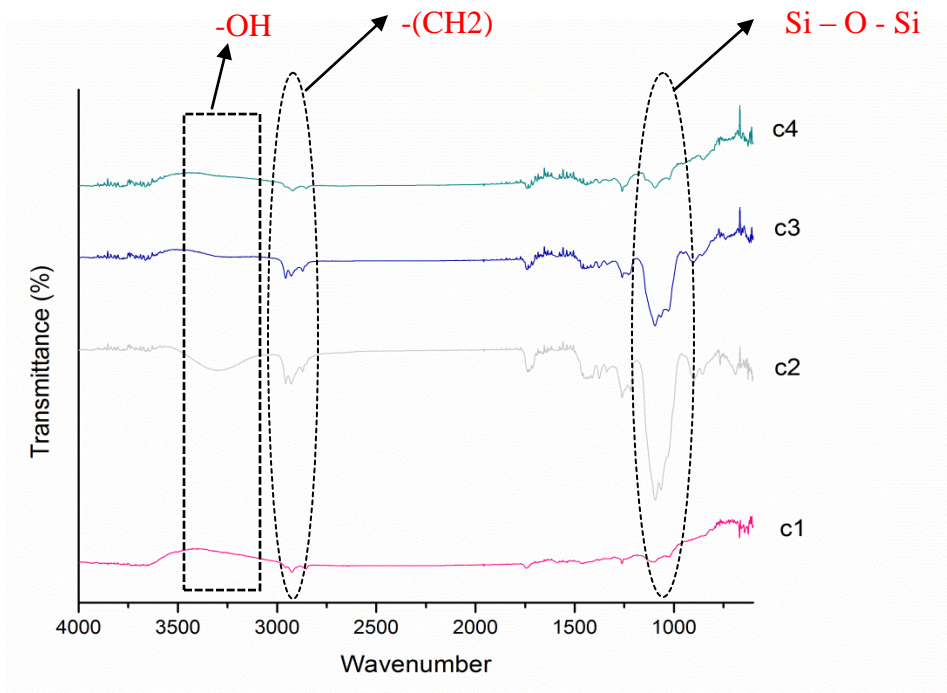


Figure 6: FTIR/ATR spectra for films of c1) PVA + EthylTMS (vol.3); c2) PVA + PropylTMS (vol.3); c3) PVA + IsobutylTMS (vol.3); c4) PVA + OctylTMS (vol.3)

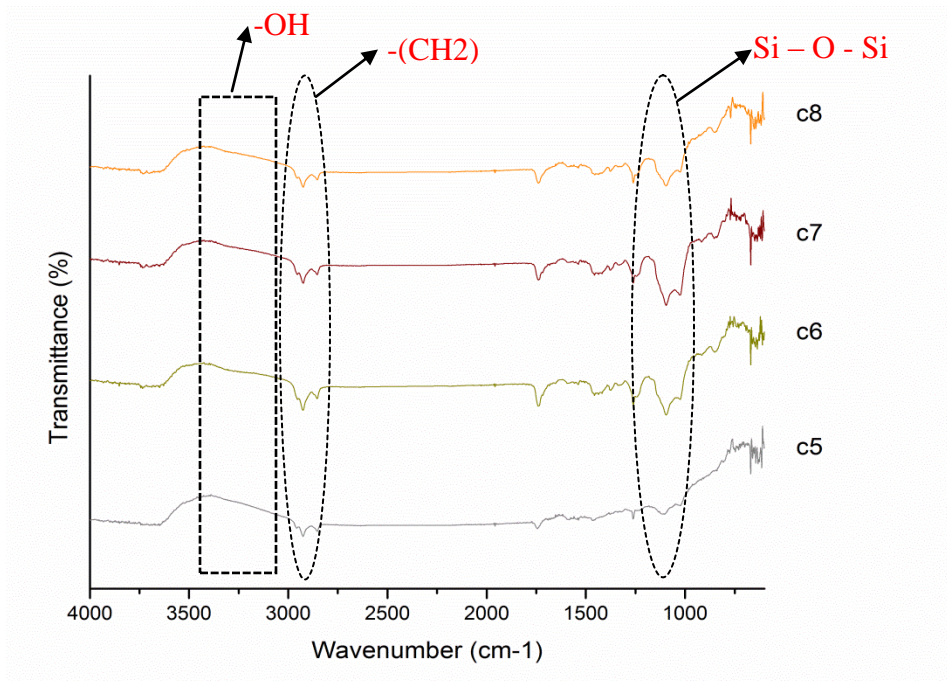


Figure 7: FTIR/ATR spectra for films of c5) PVA + EthylTMS (vol.1); c6) PVA + PropylTMS (vol.1); c7) PVA + IsobutylTMS (vol.1); and c8) PVA + OctylTMS (vol.1)

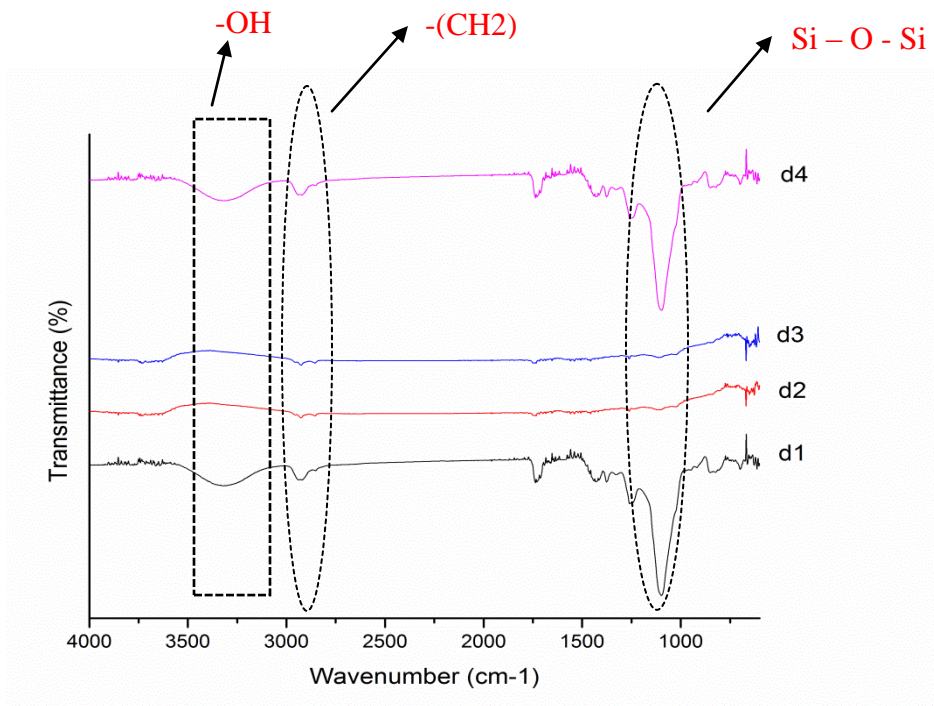


Figure 8: FTIR/ATR spectra for films of d1) PVA-Silica + EthylTMS (vol.3); d2) PVA-Silica + PropylTMS (vol.3); d3) PVA-Silica + IsobutylTMS (vol.3); d4) PVA-Silica + OctylTMS (vol.3)

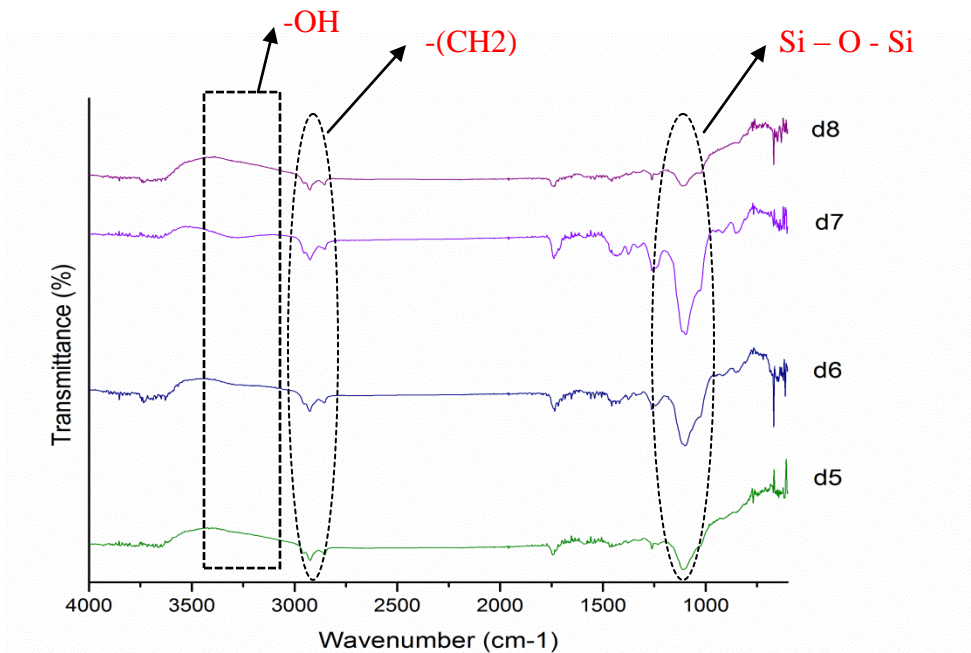


Figure 9: FTIR/ATR spectra for films of d5) PVA-Silica + EthylTMS (vol.1); d6) PVA-Silica + PropylTMS (vol.1); d7) PVA-Silica + IsobutylTMS (vol.1); and d8) PVA-Silica + OctylTMS (vol.1)

3. *Thermogravimetric analysis*

Figure 10 shows the TGA results for PVA. This figure indicates that up to 10% of the weight is lost between 30 and 270°C. During this temperature interval, two thermic effects are recognized. The first which is observed at 100°C belongs to the release of free water molecules from the nanocomposites, while the second is recognized between 270 and 450°C. The latter resembles the destruction of hydroxyl groups of PVA. A weight loss of 58.60% out of the initial weight is observed in figure 10. From the graph, 8.75% residual mass of the remaining PVA nanocomposites is recognized.

Figure 11 shows the TGA thermograph of PVA+Silica. This figure indicates that up to 10% of the weight is lost between 30 and 300°C. During this temperature interval, two thermic effects are recognized. The first which is observed at 100°C belongs to the release of free water molecules from the nanocomposites, while the second is recognized between 285 and 500°C. The latter resembles the destruction of hydroxyl groups of PVA. This thermic effect shifted 15°C higher than pure PVA nanocomposites. A 34% residual mass of silica at 500°C forming a plateau is recognized. By comparing the residual masses obtained in figures 10 and 11, the silica content that is added to the nanocomposites in figure 11 forms 25% of the remaining PVA+Silica nanocomposites. This silica amount verifies our calculations of silica from the initial mixture. Introducing alkoxysilanes to the PVA matrix shifted the thermic effects. Both figures 12 and 13 show the TGA thermograph for PVA with EthylTMS (vol. 1 and 3), PropylTMS (vol. 1 and 3), (vol. 1 and 3) and OctylTMS (vol. 1 and 3). As seen in the figure, at 100°C the first thermic effect is recognized resembling the release of free water from the nanocomposites, while the second is recognized between 300 and 500°C resembling the destruction of hydroxyl groups of PVA. This thermic effect shifted 30°C higher temperature than pure PVA nanocomposites. 20%

residual mass of silica at 500°C forming a plateau is recognized. By comparing the residual masses obtained in figures 10,12 and 13, the silanes content that is added to the nanocomposites in figures 12 and 13 forms 12% of the remaining PVA+Silica nanocomposites. This silica amount verifies our calculations of silica from the initial mixture.

Introducing alkoxy silanes to the PVA+Silica matrix also shifted the thermic effects. Figures 14 and 15 show the TGA thermograph for PVA+Silica with EthylTMS (vol. 1 and 3), PropylTMS (vol. 1 and 3), (vol. 1 and 3) and OctylTMS (vol. 1 and 3). As seen in the figures, at 100°C the first thermic effect is recognized resembling the release of free water from the nanocomposites, while the second is recognized between 310 and 500°C resembling the destruction of hydroxyl groups of PVA. This thermic effect shifted 40°C higher temperature than pure PVA nanocomposites. A 30% residual mass of silica at 500°C forming a plateau is recognized. By comparing the residual masses obtained in figures 10,14 and 15, the silanes content that is added to the nanocomposites in figure 10 forms 22% of the remaining PVA+Silica nanocomposites. This silanes amount verifies our calculations of silica from the initial mixture.

Hence, incorporating silicon dioxide and alkyl trimethoxysilanes to the PVA matrix shifted the decomposition temperature of PVA to higher temperatures. OctylTMS needed the highest temperature for decomposition, whereas EthylTMS needed the lowest temperature. Different slopes are displayed for the curves in figures 12, 13, 14 and 15 proving the existence of different decomposition temperatures. The reason for these differences is that octyl group has the largest carbon chain whereas ethyl group has the smallest carbon chain. Thus the thermal properties of the hybrid organic/inorganic nanocomposites are enhanced.

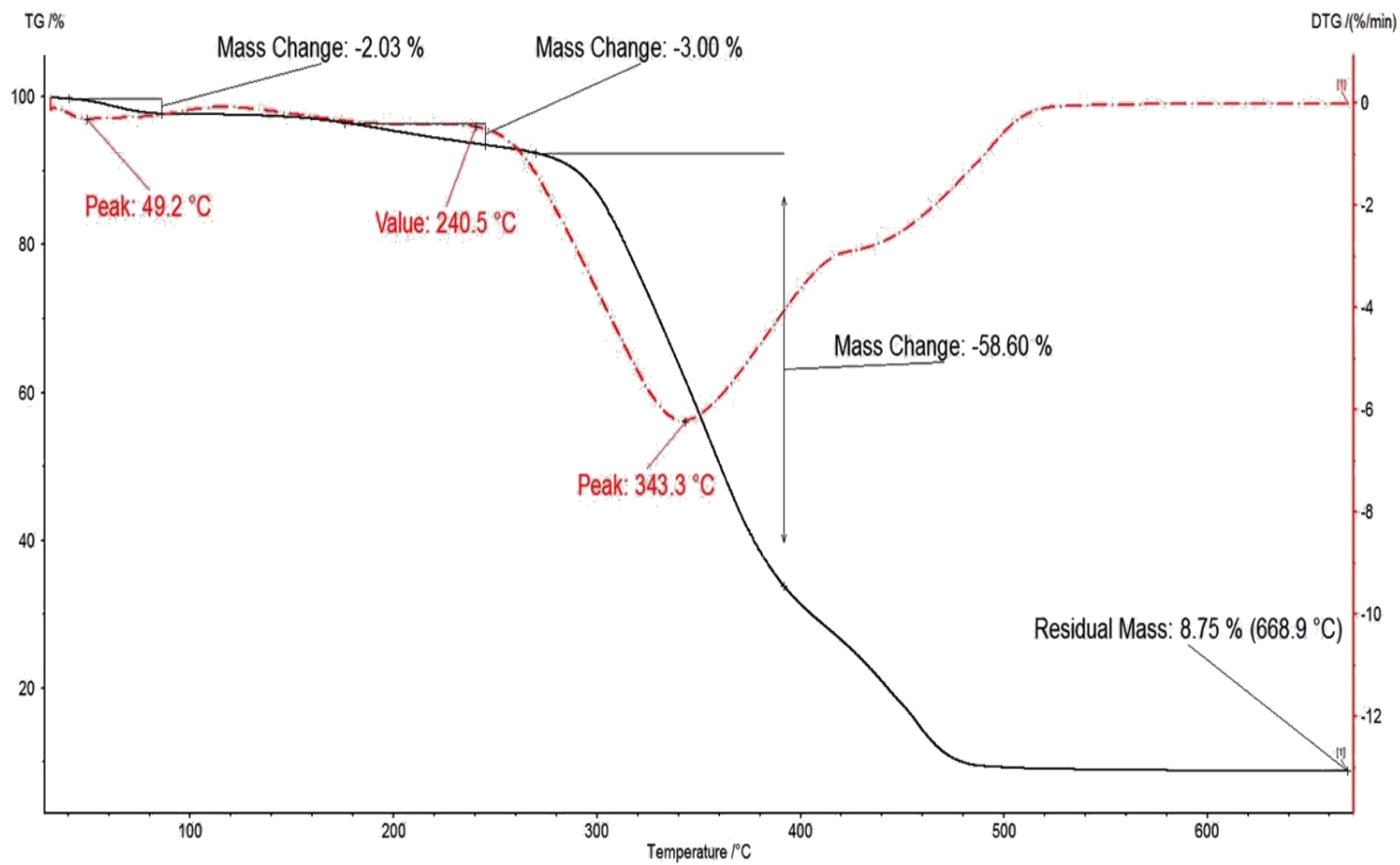


Figure 10: TGA thermograph of PVA Film

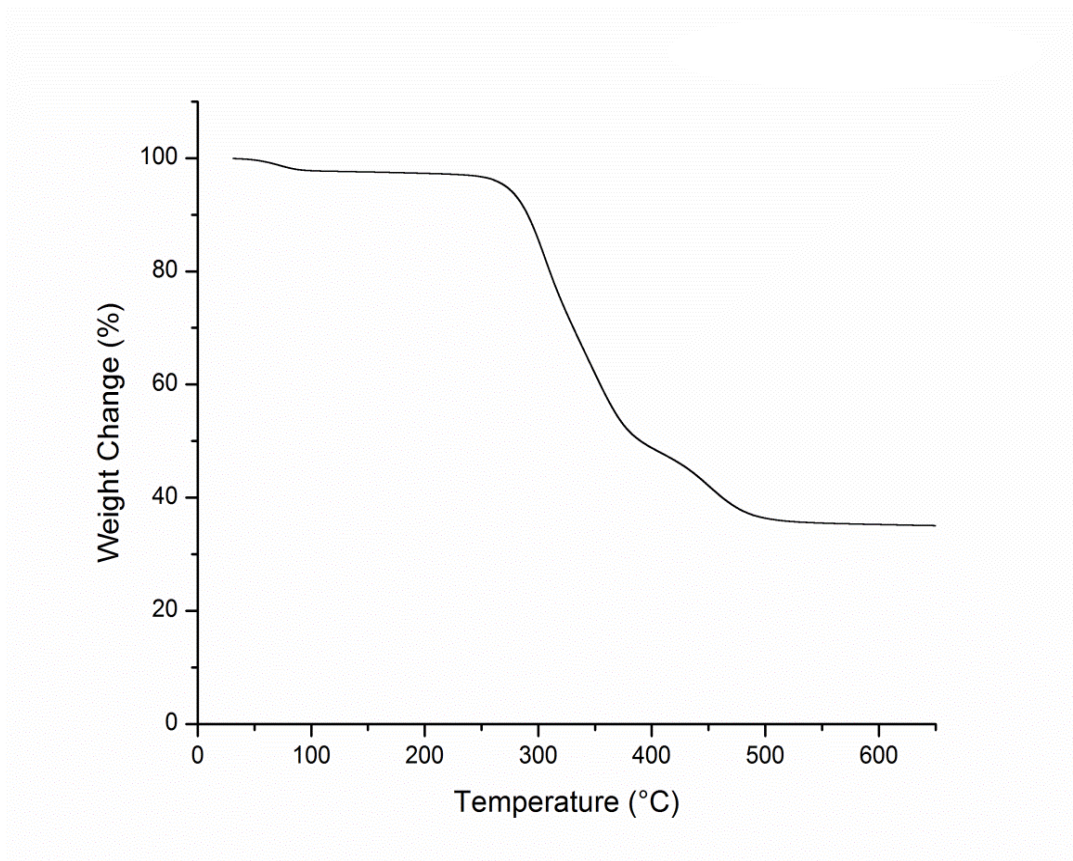


Figure 11: TGA thermograph of PVA+ Silica Film

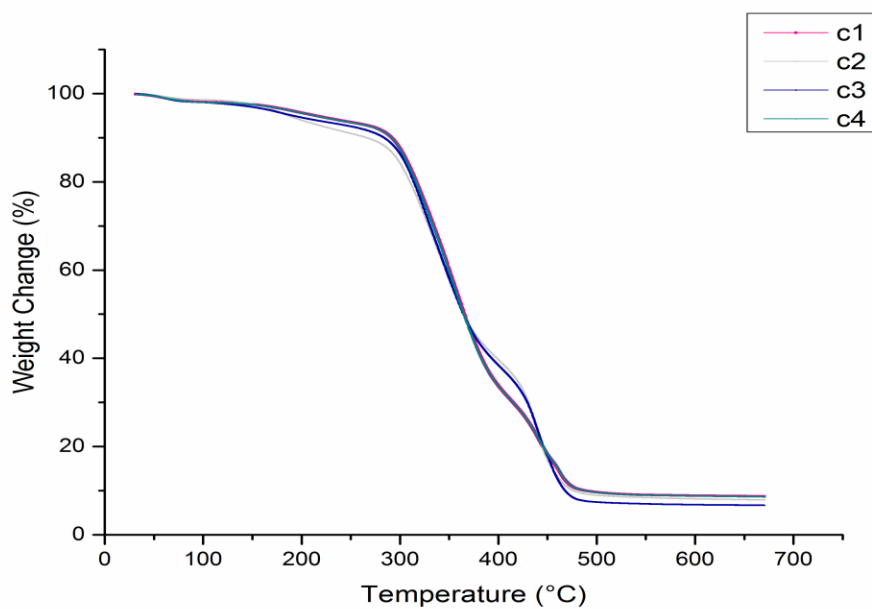


Figure 12: TGA thermograph for films of c1) PVA + EthylTMS (vol.3); c2) PVA + PropylTMS (vol.3); c3) PVA + IsobutylTMS (vol.3); c4) PVA + OctylTMS (vol.3)

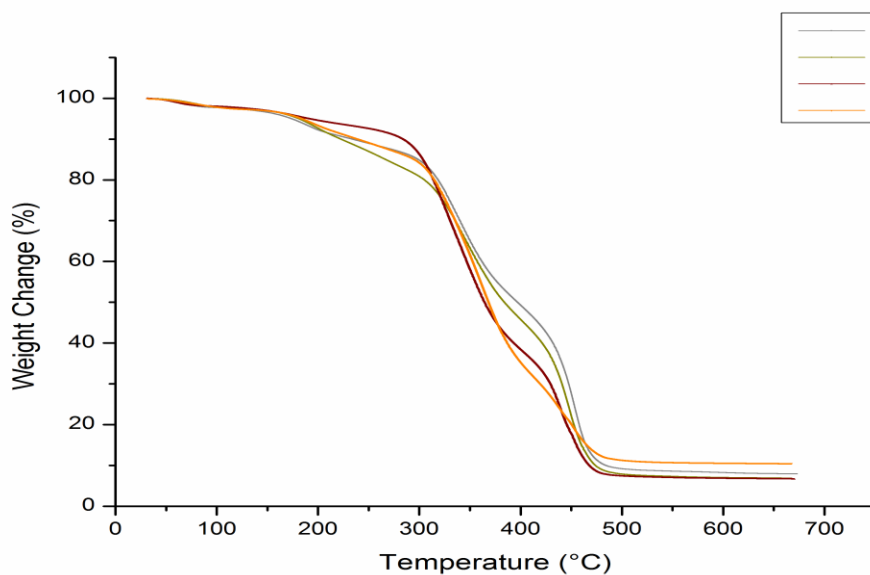


Figure 13: TGA thermograph for films of c5) PVA + EthylTMS (vol.1); c6) PVA + PropylTMS (vol.1); c7) PVA + IsobutylTMS (vol.1); and c8) PVA + OctylTMS (vol.1)

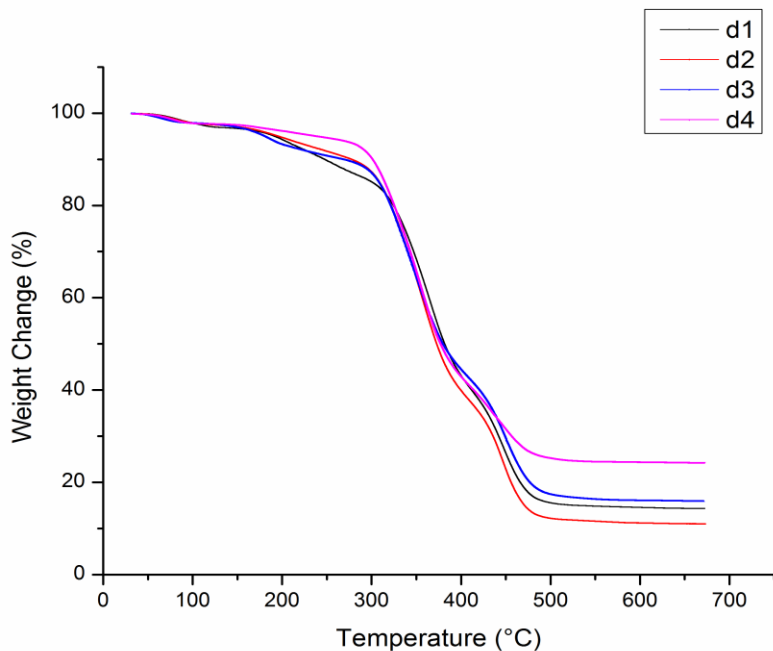


Figure 14: TGA thermograph for films of d1) PVA-Silica + EthylTMS (vol.3); d2) PVA-Silica + PropylTMS (vol.3); d3) PVA-Silica + IsobutylTMS (vol.3); d4) PVA-Silica + OctylTMS (vol.3)

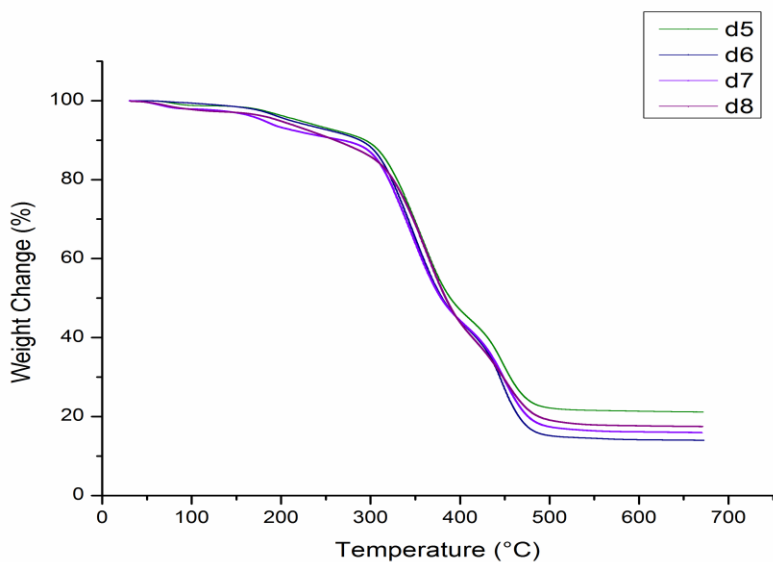


Figure 15: TGA thermograph for films of d5) PVA-Silica + EthylTMS (vol.1); d6) PVA-Silica + PropylTMS (vol.1); d7) PVA-Silica + IsobutylTMS (vol.1); and d8) PVA-Silica + OctylTMS (vol.1)

4. *Differential Scanning Calorimetry*

Glass transition (T_g), crystallization (T_c) and melting temperatures (T_m) can be obtained using DSC. Table 2 summarizes the glass transition and melting temperatures of the different obtained hybrid nanocomposites. All of the obtained hybrid nanocomposites showed no crystallization temperatures.

Glass transition temperatures were modified among the different nanocomposites. By comparing the means of the different alkyl trimethoxysilane with silica for set (vol.1), it's noticed that there are significant differences. EthylTMS (vol.1) with silica was significantly different from PropylTMS (vol.1) and OctylTMS (vol.1). IsobutylTMS (vol.1) with silica was significantly different from EthylTMS (vol.1) and OctylTMS (vol.1). OctylTMS (vol.1) was significantly different from EthylTMS (vol.1), PropylTMS (vol.1) IsobutylTMS (vol.1) and PVA. Similarly, in table 2, it's recognized that significant different were presented among the different alkyl trimethoxysilane (vol.1) without silica. Hence, the type of alkyl trimethoxysilane has an effect on the glass transition temperature, with EthylTMS having the lowest T_g and OctylTMS nanocomposites having the highest T_g . This is due to the fact that ethyl group has the shortest carbon chain while octyl group has the longest one. Pure PVA nanocomposites were taken as control group. The presence of silica had an effect in EthylTMS (vol.1), OctylTMS (vol.1) and PVA as seen in the table.

Alkyl trimethoxysilane (vol.3) with silica shows significant differences among the different types of the hybrid nanocomposites. OctylTMS (vol.3) with silica is significantly different from EthylTMS (vol.3), IsobutylTMS (vol.3), PropylTMS (vol.3) and PVA. In addition, PVA is significantly different from EthylTMS (vol.3), PropylTMS (vol.3), IsobutylTMS (vol.3) and OctylTMS (vol.1). PVA has the lowest glass transition temperature while OctylTMS (vol.3) has

the highest. Hence, an increase in the carbon chain of alkoxy silanes results in an increase in the glass transition temperature. Alkyl trimethoxysilane (vol.3) without silica displays significant differences among the various nanocomposites. The type of alkyl trimethoxysilane shifts the glass transition temperatures. PVA nanocomposites show the least temperature and OctylTMS (vol.3) without silica nanocomposites shows the highest temperature. Moreover, the presence of silica had an effect in EthylTMS (vol.1), OctylTMS (vol.1) and PVA as seen in the table.

Similarly, melting temperatures varied among the different nanocomposites. Table 2 displays the melting temperature means of the various alkyl trimethoxysilanes (vol.1 and 3) in the presence and absence of silica. Similar results to the glass transition temperature means were recognized. Increase in the carbon chain of the alkyl trimethoxysilanes increase the melting temperature. Therefore, OctylTMS nanocomposites have the highest melting temperatures among the four types of alkyl trimethoxysilanes. The presence of silica significantly affected the melting temperatures of the nanocomposite as seen in the table. All nanocomposites (vol.1 and 3) in the presence of silica demonstrated higher melting temperatures than with nanocomposites without silica. Consequently, the presence silica has a significant impact on the melting temperatures of the various hybrid nanocomposites.

Table 2: Glass transition and melting temperatures means of PVA/alkoxysilane nanocomposites

Alkoxysilane	T _g (°C)				T _m (°C)			
	With Silica	Without Silica	With Silica	Without Silica	With Silica	Without Silica	With Silica	Without Silica
	(Vol. 1)	(Vol. 1)	(Vol. 3)	(Vol. 3)	(Vol. 1)	(Vol. 1)	(Vol. 3)	(Vol. 3)
EthylTMS	39.67 ^{c,1} ±0.29	36.17 ^{d,2} ±0.29	42.67 ^{b,1} ±0.29	38.67 ^{c,2} ±0.29	172.33 ^{a,1} ±0.29	144.50 ^{a,2} ±0.50	174.67 ^{a,1} ±0.29	155.67 ^{a,2} ±0.58
PropylTMS	41.67 ^{b,1} ±0.29	41.33 ^{c,1} ±0.29	42.50 ^{b,1} ±0.50	43.00 ^{b,1} ±0.87	173.17 ^{a,b,1} ±0.29	146.83 ^{b,2} ±0.76	175.17 ^{a,1} ±0.29	162.50 ^{b,2} ±0.50
IsobutylTMS	43.00 ^{b,1} ±0.50	41.83 ^{b,1} ±0.58	44.33 ^{b,1} ±0.29	43.83 ^{b,1} ±0.29	173.67 ^{b,c,1} ±0.29	148.17 ^{c,2} ±0.29	178.83 ^{b,1} ±0.29	180.33 ^{d,2} ±0.29
OctylTMS	45.50 ^{a,1} ±0.50	44.00 ^{a,2} ±0.87	50.67 ^{a,1} ±0.76	47.00 ^{a,2} ±0.50	175.17 ^{c,1} ±0.29	149.67 ^{d,2} ±0.29	200.17 ^{d,1} ±0.29	182.50 ^{e,2} ±0.50
None	40.17 ^{b,c,1} ±0.76	26.50 ^{e,2} ±0.87	40.17 ^{c,1} ±0.76	26.50 ^{d,2} ±0.87	188.1 ^{d,1} ±0.29	164.83 ^{e,2} ±0.29	188.17 ^{c,1} ±0.29	164.83 ^{c,2} ±0.29

^{a-c} Averages in a column with different alphabetical superscripts are significantly different (P<0.05)

¹⁻² Averages in a row with different numerical superscripts are significantly different (P<0.05)

5. Water Vapor Permeability

The type of the nanocomposite, the presence of silica, and the interaction between the type of nanocomposites and presence of silica significantly affected the water vapor permeability ($p < 0.05$). IsobutylTMS (vol.3) nanocomposites were significantly different from OctylTMS (vol.3) and EthylTMS (vol.3) nanocomposites. Similarly, PropylTMS (vol.3) nanocomposites were significantly different from OctylTMS (vol.3) and EthylTMS (vol.3) nanocomposites. However, IsobutylTMS (vol.3) nanocomposites showed no significant difference from PropylTMS (vol.3) nanocomposites. Also, OctylTMS (vol.3) showed no significant difference from EthylTMS (vol.3) nanocomposites. The presence of silica increases WVTR, except for IsobutylTMS (vol.3) nanocomposites. It was proven that the interaction between the type of nanocomposites and the presence of silica had a significant impact on WVTR. Table 2 summarizes WVTR means of PVA/alkoxysilanes (vol.3) nanocomposites.

Table 3: WVTR means of PVA/alkoxysilane (vol.3) nanocomposites

Alkoxysilane	With silica ($\times 10^{-15}$)(cc/ m ² .day)	Without silica ($\times 10^{-15}$)(cc/ m ² .day)
EthylTMS (vol.3)	9.16 ^{a,b,1} \pm 0.66	5.93 ^{a,2} \pm 0.14
PropylTMS (vol.3)	9.88 ^{b,1} \pm 0.27	6.02 ^{a,2} \pm 0.17
IsobutylTMS(vol.3)	8.26 ^{a,1} \pm 0.52	10.29 ^{b,2} \pm 0.57
OctylTMS (vol.3)	11.27 ^{c,1} \pm 0.28	6.35 ^{a,2} \pm 0.89
None	11.61 ^{d,1} \pm 0.23	3.88 ^{c,2} \pm 0.23

^{a-c} Averages in a column with different alphabetical superscripts are significantly different ($P < 0.05$)

¹⁻² Averages in a row with different numerical superscripts are significantly different ($P < 0.05$)

Similarly, the type of the nanocomposite, the presence of silica, and the interaction between the type of nanocomposites and presence of silica significantly affected the water vapor permeability ($p < 0.05$). IsobutylTMS (vol.1) nanocomposites were significantly different from OctylTMS (vol.1) and EthylTMS (vol.1) nanocomposites. Likewise, PropylTMS (vol.1) nanocomposites were significantly different from OctylTMS (vol.1) and EthylTMS (vol.1) nanocomposites. However, IsobutylTMS (vol.1) nanocomposites showed no significant difference from PropylTMS (vol.1) nanocomposites. Also, OctylTMS (vol.1) showed no significant difference from EthylTMS (vol.1) nanocomposites. The presence of silica increases WVTR, except for IsobutylTMS (vol.1) nanocomposites. It was proven that the interaction between the type of nanocomposites and the presence of silica had a significant impact on WVTR. Table 3 summarizes WVTR means of PVA/alkoxysilanes (vol.1) nanocomposites.

Table 4: WVTR means of PVA/alkoxysilane (vol.1) nanocomposites

Alkoxysilane	With silica ($\times 10^{-15}$)(cc/ m ² .day)	Without silica ($\times 10^{-15}$)(cc/ m ² .day)
EthylTMS (vol.1)	13.12 ^{a,1} ±2.03	4.68 ^{a,2} ±1.06
PropylTMS (vol.1)	3.89 ^{b,1} ±0.724	5.04 ^{a,1} ±1.11
IsobutylTMS (vol. 1)	6.42 ^{b,1} ±0.47	5.34 ^{a,1} ±0.41
OctylTMS (vol.1)	12.13 ^{a,1} ±1.20	5.20 ^{a,2} ±0.11
None	11.61 ^{c,1} ±0.23	3.88 ^{a,2} ±0.23

^{a-c} Averages in a column with different alphabetical superscripts are significantly different ($P < 0.05$)

¹⁻² Averages in a row with different numerical superscripts are significantly different ($P < 0.05$)

Table 5 summarizes the permeability means of the different hybrid nanocomposites of set (vol.1) and set (vol.3). In set (vol.1) with silica, it's recognized that EthylTMS is significantly different from PropylTMS, IsobutylTMS and OctylTMS. PVA is significantly different from PropylTMS, IsobutylTMS, and OctylTMS. EthylTMS with silica (vol.1) displays similar behavior to PVA concerning water vapor permeability, whereas the rest of the alkyl trimethoxysilanes showed a decrease in the permeability of water vapor. In set (vol.3) with silica, it's detected that PVA is significantly different from EthylTMS, PropylTMS, IsobutylTMS and OctylTMS. Hence, introducing alkyl trimethoxysilanes to PVA nanocomposites decreases their permeability means. In sets (vol. 3) and (vol.1) with no silica, no significant difference exists among the different types of alkyl trimethoxysilanes. Hence, the presence of silica had no effect on the permeability means of the hybrid nanocomposites in both sets.

Table 5: Permeability means of PVA/alkoxysilane nanocomposites

Alkoxysilane	Set (vol. 1)		Set (vol. 3)	
	With Silica ($\times 10^{-10}$)(cc/m.m ² .day)	Without Silica ($\times 10^{-10}$)(cc/m.m ² .day)	With Silica ($\times 10^{-10}$)(cc/m.m ² .day)	Without Silica ($\times 10^{-10}$)(cc/m.m ² .day)
EthylTMS	3.74 ^{b,1} ±0.57	2.35 ^{a,1} ±0.53	2.41 ^{a,1} ±0.16	2.77 ^{a,1} ±0.11
PropylTMS	2.55 ^{a,1} ±0.48	2.20 ^{a,1} ±0.48	2.68 ^{a,1} ±0.11	2.13 ^{a,1} ±0.10
IsobutylTMS	2.13 ^{a,1} ±0.13	2.90 ^{a,1} ±0.20	2.65 ^{a,1} ±0.15	2.49 ^{a,1} ±0.12
OctylTMS	2.67 ^{a,1} ±0.23	2.75 ^{a,1} ±0.11	2.48 ^{a,1} ±0.57	2.65 ^{a,1} ±0.39
None	3.99 ^{b,1} ±0.13	3.10 ^{a,1} ±0.17	3.99 ^{b,1} ±0.13	3.10 ^{a,1} ±0.17

^{a-c} Averages in a column with different alphabetical superscripts are significantly different (P<0.05)

¹⁻² Averages in a row with different numerical superscripts are significantly different (P<0.05)

CHAPTER 4

CONCLUSION

PVA displays various characteristics that make it a noteworthy membrane material. Using the sol-gel technique novel hybrid organic/inorganic nano-composites were obtained. The PVA+Silica along with trimethoxysilanes nanocomposites reveals a significantly improved thermal effects. In comparison with the pure PVA, these hybrid nanocomposites exhibit higher degradation, melting and glass transition temperatures. Similar to the pure PVA, the decomposition degradation of the PVA+Silica with trimethoxysilanes nanocomposite is shown as two steps degradation. However, the integration of silanes into the PVA matrix results in modification of the degradation mechanism from that of pure PVA. Free water is eliminated in the first degradation step and hydroxyl groups are released in the second stage. The residual masses obtained resemble the silanes part. Nanocomposites add to future development in data storage, optical and pharmaceutical applications.

References

1. Al-Oweini, Rami, & El-Rassy, Houssam. (2009). Synthesis and characterization by FTIR spectroscopy of silica aerogels prepared using several Si(OR)₄ and R'Si(OR')₃ precursors. *Journal of molecular structure*, 919(1-3), 140-145.
2. Attia, Yosry A. (1994). *Sol-gel processing and applications*: Plenum Publishing Corporation.
3. Bahulekar, R. V., Prabhune, A. A., SivaRaman, H., & Ponrathnam, S. (1993). Immobilization of penicillin G acylase on functionalized macroporous polymer beads. *Polymer*, 34(1), 163-166.
4. Baker, RW. (2004). *Membrane technology and applications*. . England: John Wiley and Sons.
5. Baker, RW, Cussler, EL, Eykamp, W, Koros, WJ, Riley, RL, & Strathmann, H. (1991). Membrane separation system. *Noyes Data Corporation*.
6. Bandyopadhyay, Abhijit, Bhowmick, Anil K., & De Sarkar, Mousumi. (2004). Synthesis and characterization of acrylic rubber/silica hybrid composites prepared by sol-gel technique. *Journal of Applied Polymer Science*, 93(6), 2579-2589.
7. Bartholomew, Calvin H. (1991). Recent developments in Fischer-Tropsch catalysis. *Studies in Surface Science and Catalysis*, 64, 158-224.
8. Bartholomew, Calvin H, Pannell, Richard B, & Butler, Jay L. (1980). Support and crystallite size effects in CO hydrogenation on nickel. *Journal of Catalysis*, 65(2), 335-347.
9. Bartholomew, Calvin H, & Guzzi, L. (1991). New trends in CO activation. *Studies in surface science and catalysis*, 64, 158.

10. Beyler, Craig L, & Hirschler, Marcelo M. (2002). Thermal decomposition of polymers. *SFPE handbook of fire protection engineering*, 2.
11. Brinker, C Jeffrey, & Scherer, George W. (1990). *Sol-gel science: the physics and chemistry of sol-gel processing*: Gulf Professional Publishing.
12. Bukur, Dragomir B, & Lang, Xiaosu. (1999). Highly active and stable iron Fischer-Tropsch catalyst for synthesis gas conversion to liquid fuels. *Industrial & engineering chemistry research*, 38(9), 3270-3275.
13. Burczak, Krystyna, Gamian, Elzbieta, & Kochman, Agata. (1996). Long-term in vivo performance and biocompatibility of poly(vinyl alcohol) hydrogel macrocapsules for hybrid-type artificial pancreas. *Biomaterials*, 17(24), 2351-2356.
14. Butt, John B, Schwartz, Lyle H, Baerns, Manfred, & Malessa, Reiner. (1984). Comparison of activity and selectivity maintenance for supported iron and iron-cobalt (FeCo) Fischer-Tropsch catalysts. *Industrial & engineering chemistry product research and development*, 23(1), 51-56.
15. Cauich-Rodriguez, JV, Der, S, & Smith, R. (1996). Dynamic mechanical characterization of hydrogel blends of poly (vinyl alcohol-vinyl acetate) with poly (acrylic acid) or poly (vinyl pyrrolidone). *Journal of Materials Science: Materials in Medicine*, 7(6), 349-353.
16. Chang, In-Soung, Kim, Chi-II, & Nam, Byeong-Uk. (2005). The influence of poly-vinyl-alcohol (PVA) characteristics on the physical stability of encapsulated immobilization media for advanced wastewater treatment. *Process Biochemistry*, 40(9), 3050-3054.
17. Davies, JT, & Rideal, EK. (1963). Properties of monolayers. *Interfacial Phenomena*, 217-281.
18. Dry, ME. (1982). The SASOL route to fuels. *CHEMTECH;(United States)*, 12(12).

19. Duvenhage, DJ, Espinoza, RC, Coville, NJ, Delman, B, & Froment, G. (1994). *Catalyst Deactivation 1994*: Elsevier.
20. Finch, Christopher A. (1983). *Chemistry and technology of water-soluble polymers*: Plenum press.
21. Flory, PJ. (1969). *Principles of Polymer Chemistry* (Cornell University, Ithaca, 1953). *Statistical Mechanics of Chain Molecules*.
22. Forzatti, P, Buzzi-Ferraris, G, Morbidelli, M, & Carra, S. (1984). Deactivation of catalysts. 1. Chemical and kinetic aspects. *Int. Chem. Eng.*, 24(1), 60-73.
23. Gomes, Dominique, Nunes, Suzana P, & Peinemann, Klaus-Viktor. (2005). Membranes for gas separation based on poly (1-trimethylsilyl-1-propyne)–silica nanocomposites. *Journal of Membrane Science*, 246(1), 13-25.
24. Guzzi, L, Schay, Z, Matusek, K, & Bogyay, I. (1986). Surface structure and selectivity control in the CO+ H reaction over FeRu Bimetallic catalysts. *Applied catalysis*, 22(2), 289-309.
25. Guenet, Jean-Michel. (1992). *Thermoreversible gelation of polymers and biopolymers*: Academic Pr.
26. Harrup, M.K., Wertsching, A.K., & Stewart, F.F. (2003). Self-doped molecular composite battery electrolytes: Google Patents.
27. Hillmyer, Marc A, Lipic, Paul M, Hajduk, Damian A, Almdal, Kristoffer, & Bates, Frank S. (1997). Self-assembly and polymerization of epoxy resin-amphiphilic block copolymer nanocomposites. *Journal of the American Chemical Society*, 119(11), 2749-2750.
28. Hodgkinson, N, & Taylor, M. (2000). Thermoplastic Poly (Vinyl Alcohol)(PVOH). *Materials World*, 8, 24-25.

29. Hoh, Ka-Pi, Ishida, Hatsuo, & Koenig, Jack L. (1990). Silicon-29 solid-state nuclear magnetic resonance spectroscopy of composite interfaces. *Polymer Composites*, 11(2), 121-125.
30. Hong, Po-Da, & Miyasaka, Keizo. (1994). Structure of the amorphous phase in highly drawn poly(vinyl alcohol) fibres. *Polymer*, 35(7), 1369-1374.
31. Huang, Hao-Hsin, Orlor, Bruce, & Wilkes, Garth L. (1985). Ceramers: Hybrid materials incorporating polymeric/oligomeric species with inorganic glasses by a sol-gel process. *Polymer Bulletin*, 14(6), 557-564.
32. Huang, Hao Hsin, Orlor, Bruce, & Wilkes, Garth L. (1987). Structure-property behavior of new hybrid materials incorporating oligomeric species into sol-gel glasses. 3. Effect of acid content, tetraethoxysilane content, and molecular weight of poly (dimethylsiloxane). *Macromolecules*, 20(6), 1322-1330.
33. Huang, Y-J, & Schwarz, JA. (1987). The effect of catalyst preparation on catalytic activity: III. The catalytic activity of Ni/Al₂O₃ catalysts prepared byincipient wetness. *Applied catalysis*, 32, 45-57.
34. Ishihara, Tatsumi, Eguchi, Koichi, & Arai, Hiromichi. (1987). Hydrogenation of carbon monoxide over SiO₂ supported Fe-Co, Co-Ni and Ni-Fe bimetallic catalysts. *Applied catalysis*, 30(2), 225-238.
35. Jager, B, & Espinoza, R. (1995). Advances in low temperature Fischer-Tropsch synthesis. *Catalysis Today*, 23(1), 17-28.
36. JE., Mark. (2006). Some novel polymeric nanocomposites. *Accounts Chem Res*, 39(12), 881.

37. Jenni, A., Holzer, L., Zurbriggen, R., & Herwegh, M. (2005). Influence of polymers on microstructure and adhesive strength of cementitious tile adhesive mortars. *Cement and Concrete Research*, 35(1), 35-50.
38. Jeong, Soo-Kyeong, Jo, Yun-Kyung, & Jo, Nam-Ju. (2006). Decoupled ion conduction mechanism of poly(vinyl alcohol) based Mg-conducting solid polymer electrolyte. *Electrochimica Acta*, 52(4), 1549-1555.
39. Kobayashi, Takayoshi. (1989). *Nonlinear optics of organics and semiconductors: proceedings of the international symposium, Tokyo, Japan, July 25-26, 1988* (Vol. 36): Springer Verlag.
40. Lappalainen, Esa. (2008). *Spoken Statement*.
41. Lehtinen, E. (2000). *Book 11: Pigment coating and surface sizing of paper*: Helsinki [etc.]: Fapet Oy [etc.].
42. Lipic, Paul M, Bates, Frank S, & Hillmyer, Marc A. (1998). Nanostructured thermosets from self-assembled amphiphilic block copolymer/epoxy resin mixtures. *Journal of the American Chemical Society*, 120(35), 8963-8970.
43. Liu, Ying-Ling, Su, Yu-Huei, Lee, Kuir-Rain, & Lai, Juin-Yih. (2005). Crosslinked organic–inorganic hybrid chitosan membranes for pervaporation dehydration of isopropanol–water mixtures with a long-term stability. *Journal of membrane science*, 251(1), 233-238.
44. Liu, Zhao-Tie, Li, Yong-Wang, Zhou, Jing-Lai, & Zhang, Bi-Jiang. (1995). Intrinsic kinetics of Fischer–Tropsch synthesis over an Fe–Cu–K catalyst. *J. Chem. Soc., Faraday Trans.*, 91(18), 3255-3261.

45. Mark, J.E. , Lee, C. Y-C, & Biancini, P. A. (1995). Hybrid organic-inorganic composites. *American Chemical Society* xi, 378p.
46. Mokoena, Emma Magdeline. (2005). *Synthesis and use of silica materials as supports for the Fischer-Tropsch reaction*. Faculty of Science, University of the Witwatersrand.
47. Mulder, Marcel. (1996). *Basic Principles of Membrane Technology Second Edition*: Kluwer Academic Pub.
48. Nakane, Koji, Yamashita, Tomonori, Iwakura, Kenji, & Suzuki, Fumio. (1999). Properties and structure of poly (vinyl alcohol)/silica composites. *Journal of Applied Polymer Science*, 74(1), 133-138.
49. Noble, Richard D, & Stern, S Alexander. (1995). *Membrane separations technology: principles and applications* (Vol. 2): Elsevier.
50. Novak, Bruce M., & Davies, Caroline. (1991). "Inverse" organic-inorganic composite materials. 2. Free-radical routes into nonshrinking sol-gel composites. *Macromolecules*, 24(19), 5481-5483.
51. Oka, M., Chang, Y.-S., Nakamura, T., Ushio, K., Toguchida, J., & Gu, H.-O. (1997). SYNTHETIC OSTEOCHONDRAL REPLACEMENT OF THE FEMORAL ARTICULAR SURFACE. *Journal of Bone & Joint Surgery, British Volume*, 79-B(6), 1003-1007.
52. Oudar, Jacques. (1985). *Deactivation and poisoning of catalysts* (Vol. 20): CRC Press.
53. Peng, Fubing, Lu, Lianyu, Sun, Honglei, Wang, Yanqiang, Liu, Jiaqi, & Jiang, Zhongyi. (2005). Hybrid organic-inorganic membrane: solving the tradeoff between permeability and selectivity. *Chemistry of materials*, 17(26), 6790-6796.

54. Sanchez, C, Ribot, F, & Lebeau, B. (1999). Molecular design of hybrid organic-inorganic nanocomposites synthesized via sol-gel chemistry. *Journal of Materials Chemistry*, 9(1), 35-44.
55. Schmidt, HELMUT, Scholze, H, & Kaiser, A. (1982). Contribution to the kinetics of glass formation from solutions. *Journal of Non-Crystalline Solids*, 48(1), 65-77.
56. Schubert, Ulrich. (1996). New materials by sol-gel processing: design at the molecular level. *Journal of the Chemical Society, Dalton Transactions*(16), 3343-3348.
57. Shaw, Duncan J. (1980). Introduction to colloid and surface chemistry, 1992. *Trowbridge, Wiltshire: Redwood Books*.
58. Sinfelt, JH, Cusumano, JA, Burton, JJ, & Garten, RL. (1977). *Advanced Materials in Catalysis: Academic Press, New York*.
59. St. Pierre, RJ, & El Sayed, MA. (1987). Dependence of the reaction probability of benzene on the size of gaseous niobium clusters. *Journal of Physical Chemistry*, 91(4), 763-765.
60. Stammen, Jason A., Williams, Stephen, Ku, David N., & Guldberg, Robert E. (2001). Mechanical properties of a novel PVA hydrogel in shear and unconfined compression. *Biomaterials*, 22(8), 799-806.
61. Stre, K, W., Jasiorski, M., Ucyk, A., & Maruszewski, K. (2003). TECHNOLOGY AND APPLICATIONS OF SOL-GEL MATERIALS. *Radiation Effects and Defects in Solids*, 158(1-1), 439-450.
62. Sur, GS, & Mark, JE. (1985). Elastomeric networks cross-linked by silica or titania fillers. *European polymer journal*, 21(12), 1051-1052.

63. Uragami, Tadashi, Matsugi, Hiroshi, & Miyata, Takashi. (2005). Pervaporation characteristics of organic-inorganic hybrid membranes composed of poly (vinyl alcohol-co-acrylic acid) and tetraethoxysilane for water/ethanol separation. *Macromolecules*, 38(20), 8440-8446.
64. Uragami, Tadashi, Okazaki, Kenji, Matsugi, Hiroshi, & Miyata, Takashi. (2002a). Structure and permeation characteristics of an aqueous ethanol solution of organic-inorganic hybrid membranes composed of poly (vinyl alcohol) and tetraethoxysilane. *Macromolecules*, 35(24), 9156-9163.
65. Uragami, Tadashi, Okazaki, Kenji, Matsugi, Hiroshi, & Miyata, Takashi. (2002b). Structure and Permeation Characteristics of an Aqueous Ethanol Solution of Organic–Inorganic Hybrid Membranes Composed of Poly(vinyl alcohol) and Tetraethoxysilane. *Macromolecules*, 35(24), 9156-9163.
66. Vannice, MA. (1975). The catalytic synthesis of hydrocarbons from H₂CO mixtures over the group VIII metals: I. The specific activities and product distributions of supported metals. *Journal of Catalysis*, 37(3), 449-461.
67. Walcarius, Alain. (1998). Analytical Applications of Silica-Modified Electrodes –A Comprehensive Review. *Electroanalysis*, 10(18), 1217-1235.
68. Wang, Xuefen, Fang, Dufei, Yoon, Kyunghwan, Hsiao, Benjamin S., & Chu, Benjamin. (2006). High performance ultrafiltration composite membranes based on poly(vinyl alcohol) hydrogel coating on crosslinked nanofibrous poly(vinyl alcohol) scaffold. *Journal of Membrane Science*, 278(1–2), 261-268.
69. Wei, Y, Yang, DC, & Tang, LG. (1993). Makromol Chem Rapid Commun *Direct Link: Abstract PDF (367K) References Web of Science® Times Cited, 48.*

70. Wei, Yen, Yang, Dachuan, Tang, Liguang, & Hutchins, MaryGail K. (1993). Synthesis, characterization, and properties of new polystyrene-SiO₂ hybrid sol-gel materials. *Journal of materials research*, 8(05), 1143-1152.
71. Wen, Jianye, & Wilkes, Garth L. (1996). Organic/inorganic hybrid network materials by the sol-gel approach. *Chemistry of Materials*, 8(8), 1667-1681.
72. Witucki, Gerald L. (1993). A silane primer: chemistry and applications of alkoxy silanes. *Journal of coatings technology*, 65, 57-57.
73. Xiao, Shude, Feng, Xianshe, & Huang, Robert Y. M. (2007). Investigation of sorption properties and pervaporation behaviors under different operating conditions for trimesoyl chloride-crosslinked PVA membranes. *Journal of Membrane Science*, 302(1–2), 36-44.
74. Yan, Lu, Li, Yu Shui, & Xiang, Chai Bao. (2005). Preparation of poly (vinylidene fluoride)(pvdf) ultrafiltration membrane modified by nano-sized alumina (Al₂O₃) and its antifouling research. *Polymer*, 46(18), 7701-7706.
75. Yang, Chun-Chen, Lin, Sheng-Jen, & Wu, Gwo-Mei. (2005). Study of ionic transport properties of alkaline poly(vinyl) alcohol-based polymer electrolytes. *Materials Chemistry and Physics*, 92(1), 251-255.
76. Yen, Wei, Dachuan, Yang, & Bakthavatchalam, R. (1992). Thermal stability and hardness of new polyacrylate-SiO hybrid sol-gel materials. *Materials Letters*, 13(4), 261-266.
77. Z, Ahmad, & JE, Mark. (2001). Polyimide–Ceramic Hybrid Composites by the Sol–Gel Route. *Chem Mater* 13, 13(10), 3320.
78. Zarzycki, Jerzy. (1997). Past and Present of Sol-Gel Science and Technology. *Journal of Sol-Gel Science and Technology*, 8(1-3), 17-22.

